Advanced Aeroelasticity. Máster Universitario en Ingeniería Aeronáutica

Aeroelastic and Dynamic Structural Analysis of a non-tapered wing

Authors :
Álvaro Moral Aranda
Agustín Pérez Arjona
Vincenzo Rosciano
Álvaro Sanjuán Florido
Alfonso Velencoso Gómez

August 23, 2019

Contents

List of Figures

Chapter 1

Introduction

Structural Dynamics is a field of major importance in the design of every engineering system to deeply understand its behaviour subjected to dynamic loading. And when it comes to the concept design of aerospace structures, studying how these dynamic forces will influence the performance of the vehicle is of great interest as well.

Deeply related to the latter is the second engineering field that must be address during the early stages of aircraft design, and that is Aeroelasticity. Aeroelastic phenomena can have a significant influence on the design of flight vehicles. Indeed, these effects can greatly alter the design requirements that are specified for the disciplines of performance, structural loads, flight stability and control, and even propulsion. In addition, aeroelastic phenomena can introduce catastrophic instabilities of the structure that are unique to aeroelastic interactions and can limit the flight envelope.

The interaction between a lifting surface and the fluid field can eventually lead under certain conditions to the so-called Flutter phenomenon. Flutter is a dynamic instability, and it can be regarded as a response to a harmonic auto-excited problem with divergent oscillations in which aerodynamic forces couple with the normal modes of the structure, as a result of the interaction of elastic, inertial and aerodynamic forces.

In this document a thorough analysis of flutter will be presented, applied on a wing box which has been discretized using a FEM tool, MSC. NASTRAN, to cover both the dynamic structural analysis as well as the aeroelastic solution to flutter. Once the structural part has been detailed, a discussion about the flutter speed obtained with the Nastran SOL 145 will be presented, followed by some other solutions.

1.1 Structural model

The structure analysed is a typical aircraft wing box that has the following specifications:

- Length: 6.1 m
- Width: 1.22 m
- Mass: 3283 Kg

On the outtermost rib a pod has been installed:

- Length: 3.05 m
- Mass: 328 Kg
- Inertia: 161.7 Kgm^2

Proceeding to the FEM model, the latter has been modelled as follows:

- 66 grids.
- 60 rods.
- 20 surface elements.
- Some other rigid bars to model a pod where a missile will be later installed.

These elements can be seen in Figure 1.1:

1.2 FEM Model

- The model contains the following elements:
- GRID: it is used to define nodes in the space
- CONM2: used to define punctual masses and inertia along with their properties
- CROD: rod elements with tension, compression, and torsional capabilities.
- CQUAD4: surface element that links four nodes.
- RBAR: rigid bar element that links two nodes, being the displacement of one node dependent from the other one. RBARS elements cannot be deformed.
- RBE3: rigid element that links nodes with independent degrees of freedom and nodes with dependent degrees of freedom. It is used in order to transmit loads and mass.

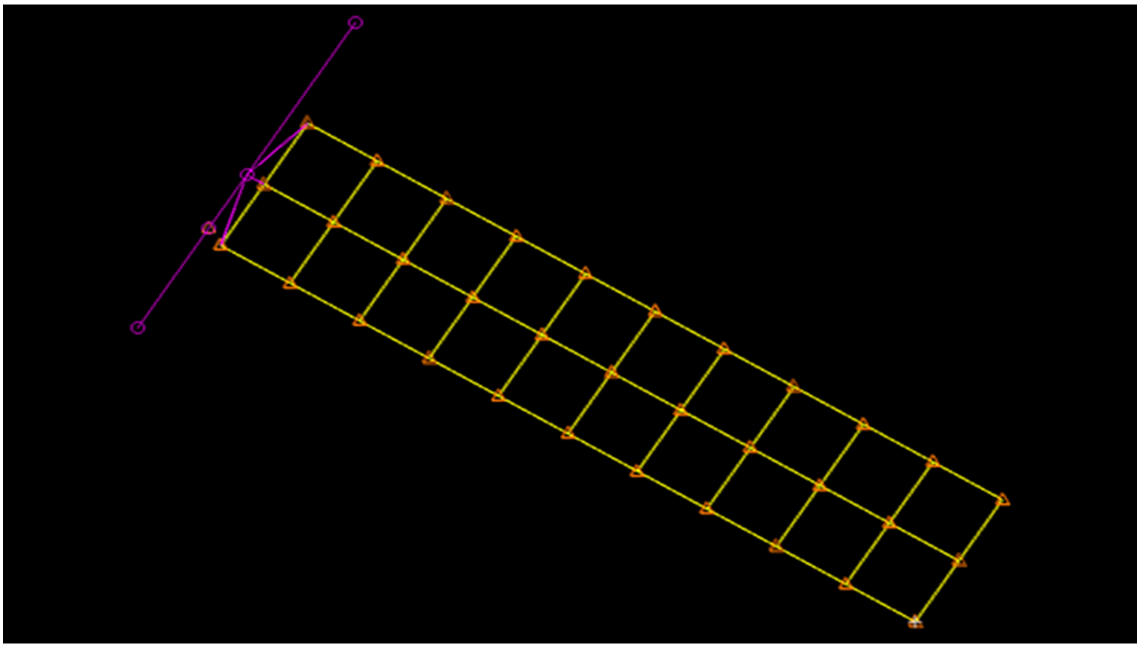

Figure 1.1: FEM Model of the wing box

- SPC: single point constraint. It is used to set boundary conditions in terms of displacements.

The reference frame used for the construction of the model has the y-axis along the wing span and the x-axis normal to it. The z-axis is perpendicular to the other two in order to obtain a right-handed triad.

Chapter 2

Normal Modes

Once the geometric and FEM model has been created, the second step was to edit the Nastran *.bdf* file to configure the solution and obtain the normal modes of vibration. For the latter, the SOL 103 command has been used.

Firstly, the wing box was clamped at the root, editing the bdf file to constrain the corresponding nodes. Secondly, the rest of the SOL 103 parameters were set to obtain the natural modes of free vibration below 50 Hz.

The equation of the system, imposing free vibration and zero damping:

$$[M]\{\ddot{u}\} + [K]\{u\} = 0 \tag{2.1}$$

And considering harmonic motion:

$$\{u\} = \{\phi\}e^{i\omega t} \tag{2.2}$$

$$([K] - \omega^2[M])\{\phi\} = 0 \tag{2.3}$$

Finding the non-trivial roots of this determinant poses an eigenvalue problem, where $\lambda = \omega^2$. Nastran solves it finding the eigenvalues to calculate the normal modes.

To extract these eigenvalues the Lanczos method has been set as parameter of the SOL 103 configuration. The fringe of each mode obtained by running the solution is presented in the next section, along with its natural frequency.

2.1 Fringe representation of normal modes

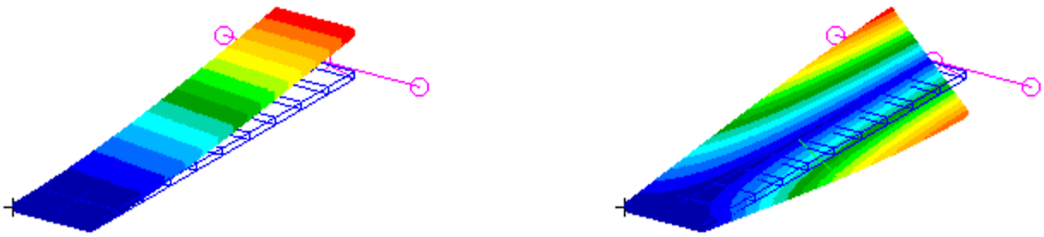

(a) Mode 1. First plunge.
$f_n = 1.56 H_z$

(b) Mode 2. First torsion.
$f_n = 2.25 H_z$

Figure 2.1: Modes 1 and 2

(a) Mode 3. Plunge and torsion I.
$f_n = 6.99 H_z$

(b) Mode 4. Plunge around z axis.
$f_n = 8.78 H_z$

Figure 2.2: Modes 3 and 4

(a) Mode 5. Plunge and torsion II.
$f_n = 9.71 H_z$

(b) Mode 6. Plunge and torsion III.
$f_n = 12.12 H_z$

Figure 2.3: Modes 5 and 6

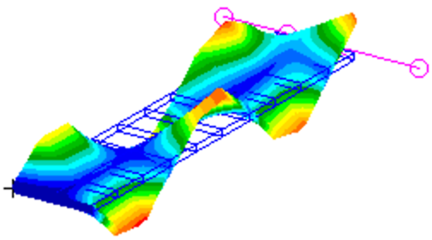

(a) Mode 7. Plunge and torsion IV.
$f_n = 17.08H_z$

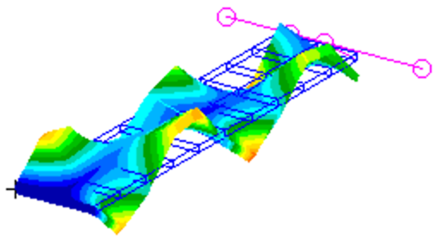

(b) Mode 8. Plunge and torsion V.
$f_n = 21.18H_z$

Figure 2.4: Modes 7 and 8

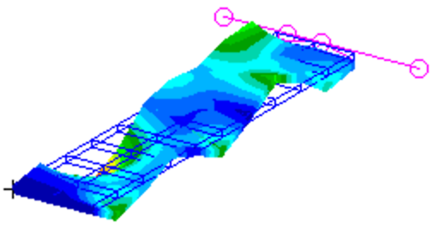

(a) Mode 9. Plunge and torsion VI.
$f_n = 24.62H_z$

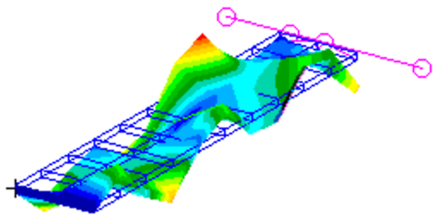

(b) Mode 10. Plunge and torsion VII.
$f_n = 25.67H_z$

Figure 2.5: Modes 9 and 10

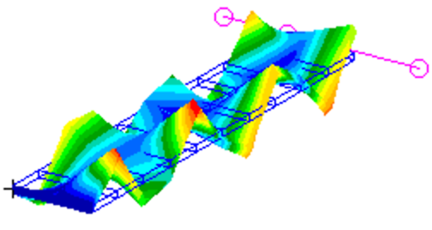

(a) Mode 11. Plunge and torsion VIII.
$f_n = 28.62H_z$

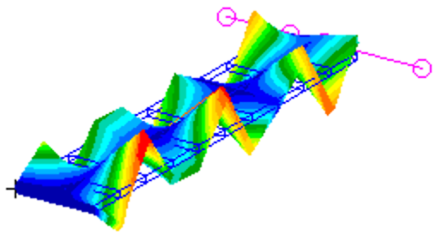

(b) Mode 12. Plunge and torsion IX.
$f_n = 31H_z$

Figure 2.6: Modes 11 and 12

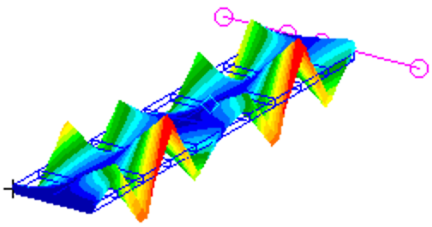

(a) Mode 13. Plunge and torsion X.
$f_n = 32.8H_z$

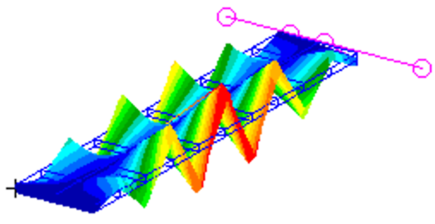

(b) Mode 14. Plunge and torsion XI.
$f_n = 33.87H_z$

Figure 2.7: Modes 13 and 14

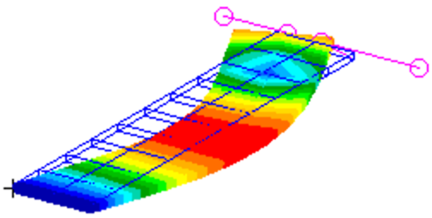

(a) Mode 15. Plunge and torsion XII.
$f_n = 38.25H_z$

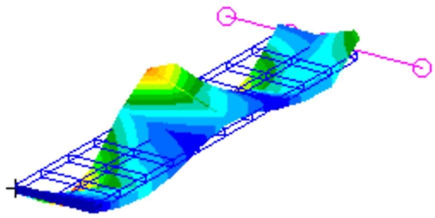

(b) Mode 16. Plunge and torsion XIII.
$f_n = 41.98H_z$

Figure 2.8: Modes 15 and 16

Chapter 3

Flutter Equation

It is of great importance to know which are the flight conditions under which the structure suffers instabilities such as divergence or flutter.

In order to find them, a dynamic analysis must be carried out. The equation of a dynamic system with damping can be expressed as follows:

$$[M_{aa}]\{\ddot{u}_a(t)\} + [B_{aa}]\{\dot{u}_a(t)\} + [K_{aa}]\{u_a(t)\} = \{P_a(t)\} \tag{3.1}$$

Where u_a is the vector of nodal displacements of the a-set, M_{aa} is the a-set mass matrix, B_{aa} is the a-set damping matrix, K_{aa} is the a-set stiffness matrix and P_a is the a-set vector of nodal aerodynamic forces.

P_a can be expressed as a function of the nodal displacements as well:

$$\{P_a(t)\} = q_\infty \int_0^t \left[H_{aa}\left(\frac{2U_\infty}{c}(t-\tau), M_\infty \right) \right] \{u_a(\tau)\} d\tau, \tag{3.2}$$

where q_∞ is the dynamic pressure($q_\infty = \frac{1}{2}\rho_\infty U_\infty^2$) and H_{aa} is the step response of the system for each nodal displacement.

In order to simplify the analysis, the nodal displacements will be considered to be a combination of the modes of free vibration ϕ_{ah}.

$$\{u_a(t)\} = [\phi_{ah}]\{u_h(t)\} \tag{3.3}$$

Where $u_h(t)$ are the modal displacements or modal coordinates.

The modes used are the ones below 50 Hz obtained in the previous section. It is considered that those modes approximate well enough the nodal displacements, as flutter is a low frequency phenomenon.

The dynamic equation multiplied by ϕ_{ah}^T:

$$\begin{aligned}&[\phi_{ah}^T][M_{aa}][\phi_{ah}]\{\ddot{u}_h\} + [\phi_{ah}^T][B_{aa}][\phi_{ah}]\{\dot{u}_h\} + [\phi_{ah}^T][K_{aa}][\phi_{ah}]\{u_h\}\} = \\ &q_\infty \int_0^t [\phi_{ah}^T]\left[H_{aa}\left(\frac{2U_\infty}{c}(t-\tau), M_\infty\right)\right][\phi_{ah}]\{u_h(\tau)\}d\tau\end{aligned} \tag{3.4}$$

Or expressing it in terms of the generalized stiffness, mass and aerodynamic response matrices:

$$\begin{aligned}&[M_{hh}]\{\ddot{u}_h(t)\} + [B_{hh}]\{\dot{u}_h(t)\} + [K_{hh}]\{u_h(t)\}\} = \\ &q_\infty \int_0^t \left[Q_{hh}\left(\frac{2U_\infty}{c}(t-\tau), M_\infty\right)\right]\{u_h(\tau)\}d\tau\end{aligned} \tag{3.5}$$

There are different methods to solve these equations. Some of them allow to obtain more accurate results than others but at higher computational cost. A quick method is the so-called K-method or V-g method.

3.1 K Method

The main idea of this method is that flutter occurs when one mode reaches simple harmonic motion, i.e. when the real part of the eigenvalue is 0 (zero damping), while the rest of the modes are still convergent (damped modes). Keeping in mind this idea, a way to find the boundary between stable and unstable (the flutter boundary) behaviour is by assuming harmonic motion.

$$u_h(t) = \hat{u}_h e^{i\omega t} \tag{3.6}$$

Another fundamental reason to do this is that non-steady aerodynamic forces are very difficult to calculate. In order to avoid this difficulty, recalling the already mentioned idea about harmonic motion and flutter, it can be assumed that aerodynamic forces are also harmonic, which are well known. To study the system motion in the frequency domain a Laplace transformation is applied to equation 3.5:

$$\left(-\omega^2[M_{hh}] + i\omega[B_{hh}] + [K_{hh}] - q_\infty\left[Q_{hh}\left(\frac{2U_\infty}{c}\omega, M_\infty\right)\right]\right)\{u_h(\omega)\} = 0 \tag{3.7}$$

Where $\{u_h(\omega)\}$ and $[Q_{hh}(\frac{2U_\infty}{c}\omega, M_\infty)]$ are the Laplace transforms of $\{u_h(t)\}$ and $[Q_{hh}(\frac{2U_\infty}{c}t, M_\infty)]$.

A few comments are remarkable in order to explain how damping is modeled:

- It is assumed that the model has no damping, although it is known that it has a structural damping of 0,03.
- The K method assumes an artificial damping (g) in the sense that it is not a physical damping present in the structure, but the damping that the structure would require in order to have harmonic motion as it was assumed before.
- When this artificial damping it is calculated, it is compared with the real one. If the artificial damping is bigger than the real one, that means that the damping required to force harmonic motion it is higher than the damping that the structure has, so the motion will be unstable. On the other hand, if the artificial damping is lower than the real one, that means that the structure has enough damping to make the motion convergent.

$$[B_{hh}] = \frac{g_{hh}}{\omega}[K_{hh}] \tag{3.8}$$

Introducing the reduced frequency $k = \frac{c\omega}{2U_\infty}$, where c is the wing chord:

$$\left(\left(\frac{2kU_\infty}{c}\right)^2 [M_{hh}] - (ig_{hh} + 1)[K_{hh}] + \frac{1}{2}\rho_\infty U_\infty^2 [Q_{hh}(k, M_\infty)]\right)\{u_h\} = 0 \tag{3.9}$$

As the trivial solution has no interest, the flutter solution is the one that makes the determinant equal to zero:

$$\det\left(\left(\frac{2kU_\infty}{c}\right)^2 [M_{hh}] - (ig_{hh} + 1)[K_{hh}] + \frac{1}{2}\rho_\infty U_\infty^2 [Q_{hh}(k, M_\infty)]\right) = 0 \tag{3.10}$$

The latter is the flutter equation of the wing. As it is a complex equation, the reduced frequency of each mode (k) and the structural damping required to have harmonic motion for each mode (g) are obtained as a function of the flight conditions. If the g obtained is greater than the actual structural damping ($g_{structure}$), the response will be unstable. If it is lower, it will be stable. Therefore the intersections between the (V-g) curve and $g = g_{structure}$ shows where the system becomes unstable. Their corresponding flight conditions are the ones associated to the beginning of flutter and must be avoided during flight.

The generalized mass and stiffness matrices have been obtained during the modal analysis of the structure. The eigenvectors have been normalized so that the normalized mass matrix becomes the identity. Since the eigenvectors satisfy the condition of orthogonality, the stiffness matrix is also diagonal. Both of them are shown below in the form of pseudovectors, meaning the diagonal of the matrix.

$$M_{hh} = \begin{bmatrix} 1 \\ 1 \\ 1 \\ 1 \\ 1 \\ 1 \\ 1 \\ 1 \\ 1 \\ 1 \\ 1 \\ 1 \\ 1 \\ 1 \\ 1 \\ 1 \end{bmatrix} kg$$

$$K_{hh} = \begin{bmatrix} 9.582 \cdot 10 \\ 1.997 \cdot 10^2 \\ 1.929 \cdot 10^3 \\ 4.044 \cdot 10^3 \\ 3.722 \cdot 10^3 \\ 5.803 \cdot 10^3 \\ 1.151 \cdot 10^4 \\ 1.771 \cdot 10^4 \\ 2.393 \cdot 10^4 \\ 2.600 \cdot 10^4 \\ 3.234 \cdot 10^4 \\ 3.796 \cdot 10^4 \\ 4.247 \cdot 10^4 \\ 4.530 \cdot 10^4 \\ 5.775 \cdot 10^4 \\ 5.956 \cdot 10^4 \end{bmatrix} \frac{N}{m}$$

The matrix containing the generalized aerodynamic forces $Q_{hh}(k, M_\infty)$ has been calculated running the Nastran SOL 145 algorithm, which for this case Doublet-Lattice theory has been applied on every panel section over the wing. The parameter configuration has been described in section 9.1.

3.2 Static instability: Divergence

After obtaining the flutter equation (3.10) the divergence equation can be easily obtained. It is only necessary to make $k = 0$, as the static case has a null frequency. Later on, the V-g method results will be shown and this instability will be identified as it is the one with $k = 0$.

Chapter 4

PK Matched Diagram

In order to obtain the flutter boundary, that is, the velocity at which the phenomenon of flutter starts, several mathematical methods can be used. For the present report, the PK method has been applied. It combines the idea of two methods:

- The P method: It solves the equation of flutter directly with non-steady aerodynamics theories and the unknowns are the real and imaginary parts of the eigenvalues. It is known from literature to be the most accurate procedure, but it has the disadvantage that it is not always possible to calculate the unsteady aerodynamic forces.

- The K method: Explained in the previous section. Harmonic motion and harmonic aerodynamic forces are assumed as a simplification.

In 1971, Hassig demonstrated that the aproximation of harmonic motion and harmonic aerodynamics forces used in the K method was inadequate in some cases in which the predictions were wrong. However, the PK method solved this problem relaxing the hypothesis of harmonic motion, assuming only harmonic aerodynamics forces.

The free-stream air speed U_∞ is obtained as a function of the free-stream density ρ_∞ and Mach number M_∞, according to the International Standard Atmosphere. Therefore, the result obtained is a PK-Matched Diagram.

Nastran has been used to carry out the flutter analysis by using the PKNL method. The studied case is a cruise flight at $M_\infty = 0.8$ and altitude within the range [0km$<$h$<$32km]. Further details can be read in the appendix where the .bdf file is included for Nastran analysis.

The following diagrams have been obtained:

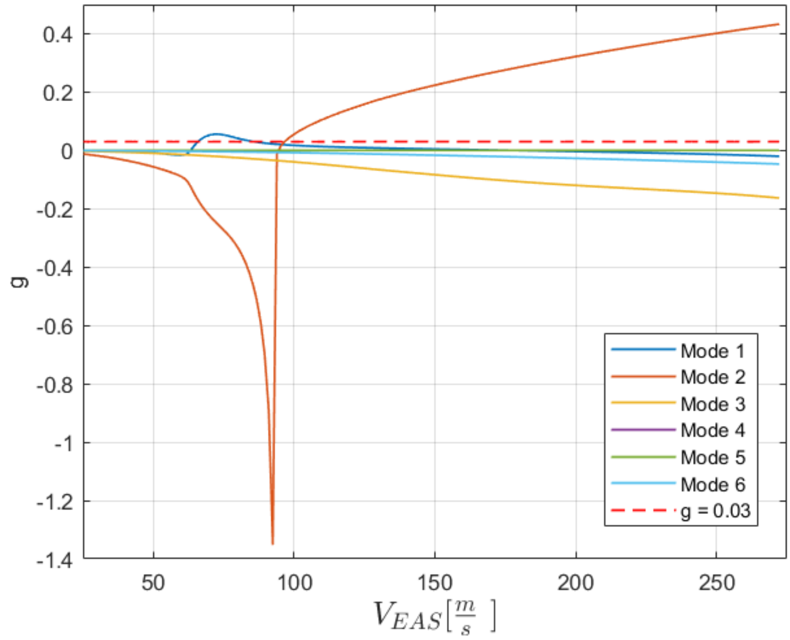

Figure 4.1: V-g diagram

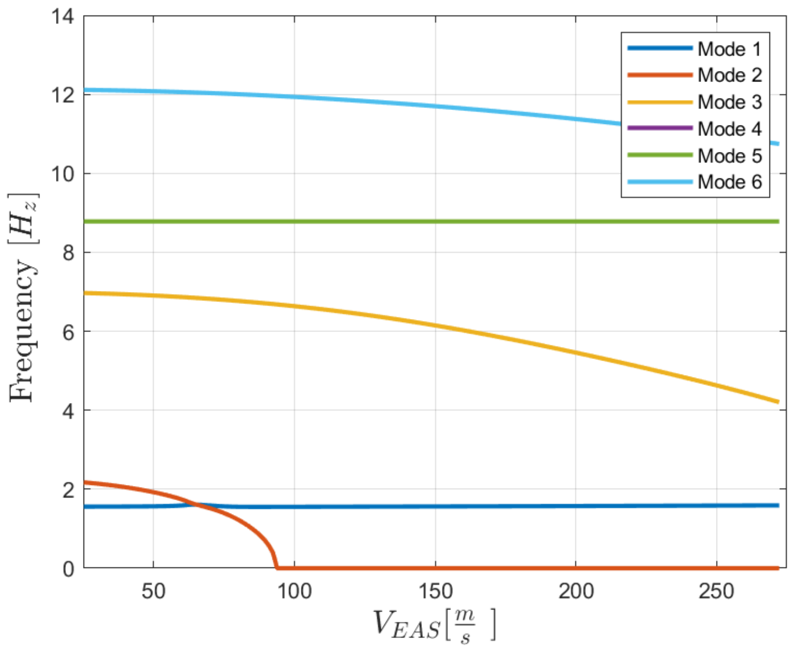

Figure 4.2: V-f diagram

Figure 4.1 shows the relation between g and V_{EAS} and figure 4.2 shows the relation between harmonic oscillation frequency and V_{EAS} for the first 6 modes of vibration.

4.1 Flutter

The parameter g can be considered as an artificially structural damping. As mentioned previously, it is the required value of structural damping to have harmonic motion. The flutter boundary begins at $V_{EAS}|_{flutter} = 65.8\frac{m}{s}$, where the damping of the first mode is equal to 0.03 (see figure 4.1), which is the real structural damping ($g_{structure}$). Sometimes, flutter is described as a phenomenon of energy transfer between modes [2], which starts being critical when their two frequencies coalesce. This behaviour is shown in the V-f diagram (4.2), where the frequency of the second mode approaches the first one until they are equal for $V_{EAS} \simeq V_{EAS}|_{flutter}$. It is remarkable to say that a first step in order to avoid flutter is to separate the frecuencies of the modes that coalesce.

The flutter boundary obtained can be physically regarded as a complete dynamic interaction between the wing structure and airflow. For any value of speed less than $V_{EAS}|_{flutter} = 65.8\frac{m}{s}$, any disturbance of the wing gets damped with exponentially decreasing amplitudes. It could be said that air provides the required damping to attenuate the disturbance. Above the flutter speed, however, the air provides the sufficient negative damping, and instead of decreasing the oscillatory motion created by the disturbance, the amplitude starts increasing exponentially.

In some cases, increasing speed after $V_{EAS}|_{flutter}$ will continuously increase g and the system will diverge faster. With this wing, if V_{EAS} is high enough, g decreases and gets into the stable region again (below the red dashed line). This event happens at $V_{EAS} = 85.8\frac{m}{s}$.

4.2 Divergence

The V-g curve for the second mode shows a singularity at $V_{EAS} = 93.9\frac{m}{s}$, where g goes from having a big margin of stability to the unstable region. At the same V_{EAS}, its frequency becomes equal to zero (see 4.2). Therefore this instability is considered to be a static divergence.

Chapter 5

Joining Wing and Pod with Springs.

Initially, the junction between wing and pod has been considered to be rigid. The previous results have been obtained with that configuration. In this chapter, the pod has been joined to the external wing rib by installing springs in the degrees of freedoms of vertical displacement (along z-axis) and torsion (around y-axis). The rest of degrees of freedom will be joined in a rigid way. From now on, the value of the stiffness of each spring will be called k_v for the longitudinal one, and k_θ for the torsional one. Both of them are ideal springs with natural elongation equal to zero. Figure 5.1 shows the joined grids with springs. Grid 20005 is part of the external wing rib and Grid 20001 belongs to the pod.

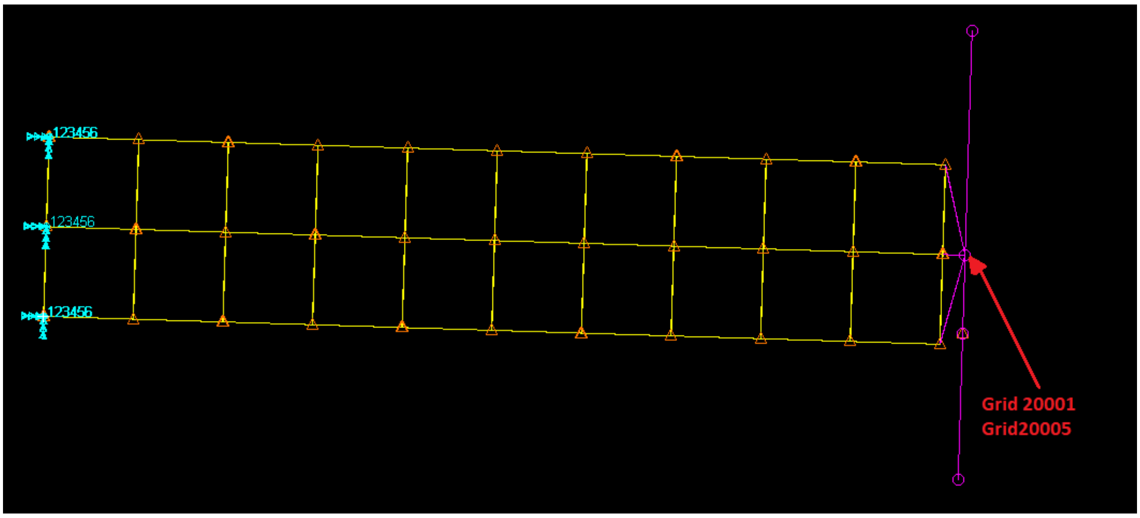

Figure 5.1: Wing-Pod Joint

The Bulk Data Entry of Nastran used to model the connections between both modes are CELAS2 for the degrees of freedom with springs, and MPC for the rigid connections (see Fig. 5.2).

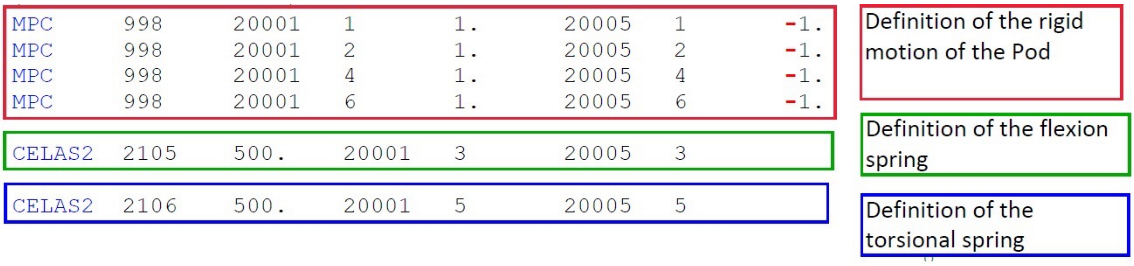

Figure 5.2: Section of bdf file to model connection with springs

5.1 Effects of spring stiffness on natural frequencies.

In order to illustrate the effect of the springs on the structure, the first four natural frequencies have been calculated for a range of values of k_v and k_θ. Figure 5.3 shows the frequencies for a given value of k_θ and a wide range of k_v. Figure 5.4 and 5.5 show the effect of both stiffness on the first and second natural frequency.

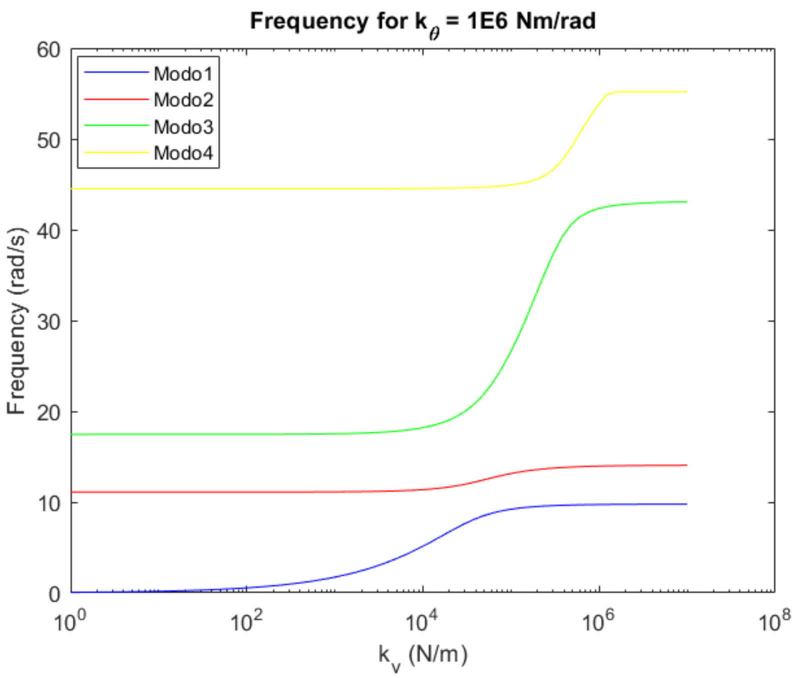

Figure 5.3: First four modes Frequencies-k_v for $k_\theta = 10^6$

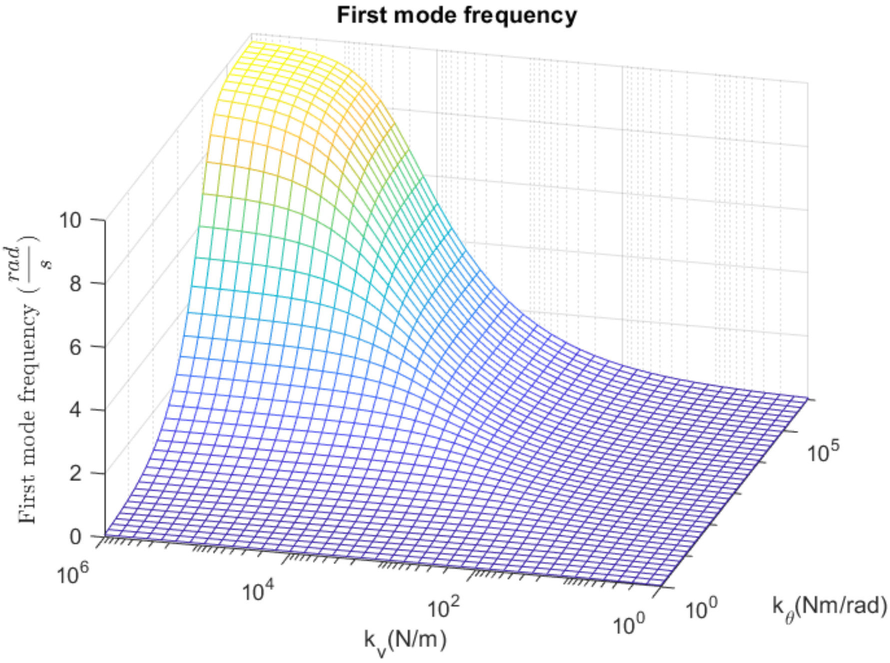

Figure 5.4: Influence of k_v and k_θ on the first mode frequency

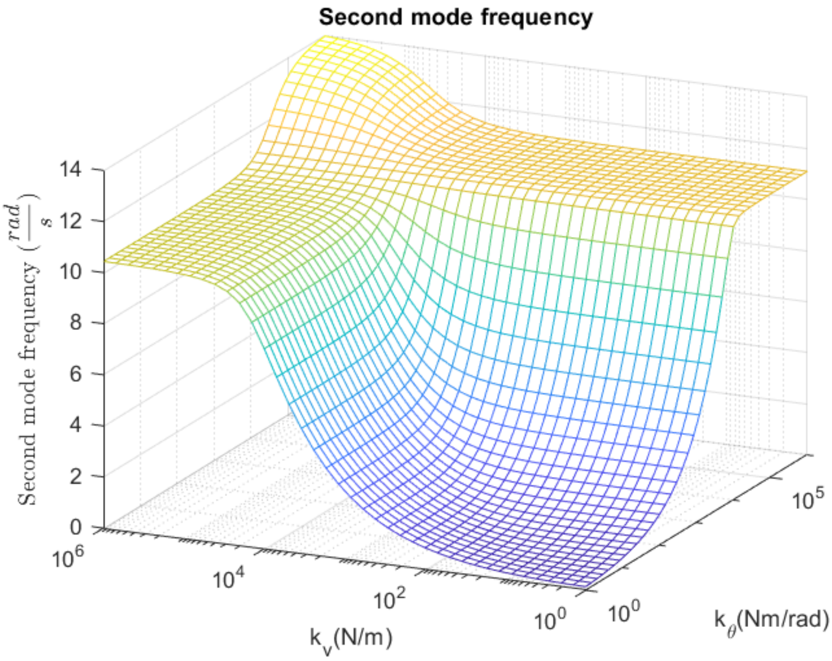

Figure 5.5: Influence of k_v and k_θ on the second mode frequency

Frequencies have horizontal asymptotes for great values of k_v and k_θ. Their asymptotic

values are the ones obtained in chapter 2, which means that by increasing the stiffness of the joints, the frequencies approach the values of the rigid joint case (first mode is plunge and second mode is torsion). For $k_v \geq 10^5 N/m$ and $k_\theta \geq 10^5 Nm/rad$, the frequencies have values very close to the ones of the rigid joint configuration.
The lower values obtained correspond to the natural frequencies of the springs, that makes sense because for very low k values, the frecuency mode is proportional to $\sqrt{k}$.
The intermediate values in the plot of second mode (flat part of the plot) correspond to the frequency of the plunge mode. This is because one stiffness is still very low and the first mode is approximately the natural frecuency of that spring. However, as it was said, when both stiffness values are high enough, the frequencies of mode 2 now tend to that of the torsion mode, and the values of mode 1 tend to the plunge mode.

5.2 Study of pod vibrations.

One of the goals of this analysis report was to find the values for k_v and k_θ so that the vibration amplitude of the pod would be smaller than the ones obtained at the wing. As it is shown below, this is not possible, as the vibrations of the pod are always bigger than those of the wing.

5.2.1 Effects of spring stiffness on the pod vibration amplitude.

The motion of the whole structure is influenced by the values of the stiffness. In the previous section, the influence on natural frequencies was studied. Now, the focus will be on the ratio of vibration amplitude between the tip of the wing and the pod. A comparison between displacements for grids 20001 (pod) and 20005 (tip of the wing) has been made for the first modes using different stiffness. These results are shown in figures 5.6 and 5.7 .

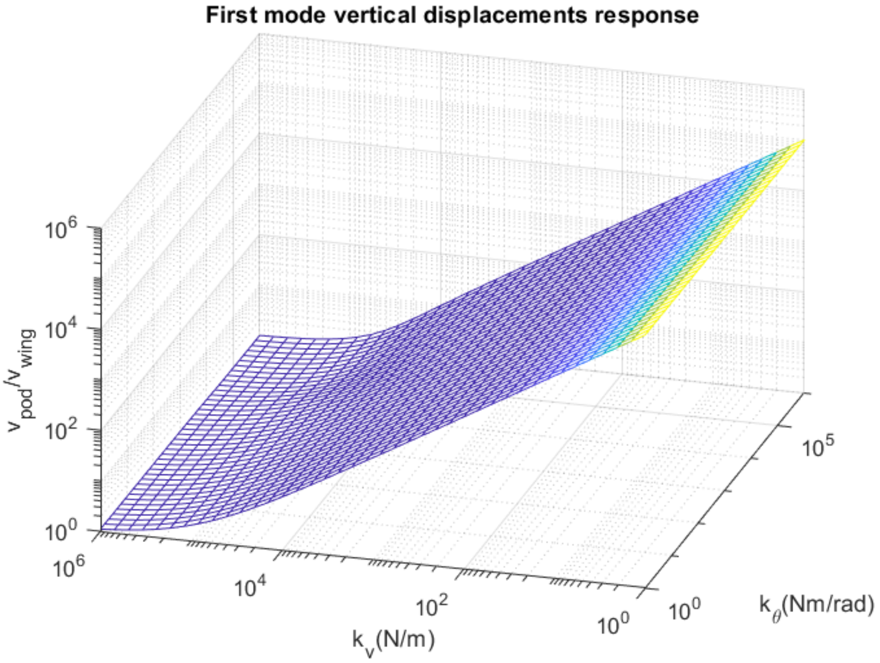

Figure 5.6: Ratio of vertical displacements in plunge mode as a function of k_v and k_θ

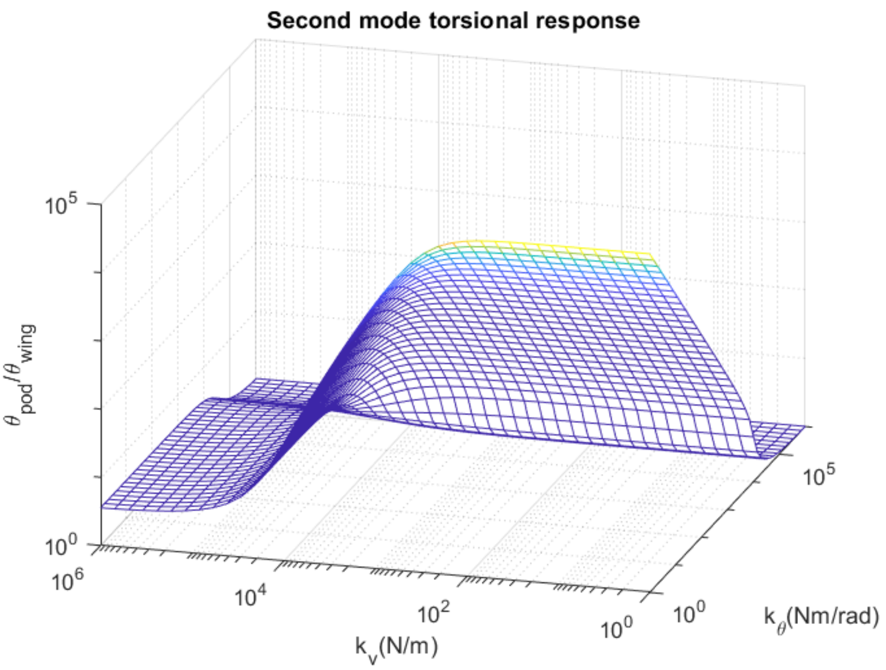

Figure 5.7: Ratio of spins in torsion mode as a function of k_v and k_θ

Both figures show that the pod motion will be greater in terms of vertical displacement and spin than the wing motion for any values of k_v and k_θ. The minimum is found when both k_v and k_θ are extremely high, which means rigid joint. In that case, both ratios are equal to 1.

Therefore, these springs have no use if the goal is to reduce the vibrations of the pod. However, they can be used to reduce wing vibrations and improve flutter behaviour as it will be explained in the next sections.

5.3 Analysis of wing vibrations.

There is plenty of information regarding the theory of dynamics in order to decrease vibrations on any system. One of the most popular approaches is the theory of *mass damper*, which could be used to reduce the vibration amplitude under certain conditions.

The wing-pod system can be regarded as one with a mass damper. In this case, the pod acts as the mass damper while the wing is the system whose vibrations need to be reduced.

5.3.1 Mass damper.

Structures with small damping as this one, may develop vibrations of big amplitudes for loads acting at frequencies close to resonance. This response can be reduced by connecting a mass through a spring and a damper whose values shall be tuned. The original idea of the tuned mass damper belongs to Frahm [1], who did only include a spring but not a damper in his mass damper design.

In this section, a mass damper design will be proposed for the model. The pod will be attached with 2 springs but without dampers, since this is a design requirement. However, if a damper was introduced, it would be more effective reducing vibrations.

Figure 5.8, shows the configuration for a single degree of freedom problem.

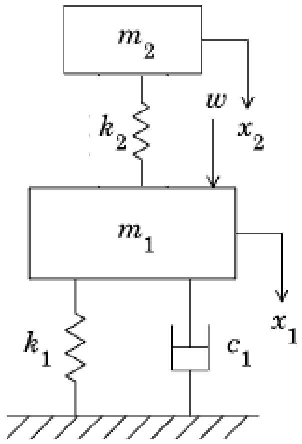

Figure 5.8: Dynamic vibration absorber attached to a single degree of freedom system [3]

In the studied case, the main body (m_1) whose vibrations need to be reduced would be the wing, while the pod would act as the mass damper (m_2).

A similar configuration was studied in [3], where the vibration amplitude is obtained as a function of the mass ratio ($\mu = \frac{m_2}{m_1}$), the natural frequencies ($\omega_1 = \sqrt{\frac{k_1}{m_1}}$ and $\omega_2 = \sqrt{\frac{k_2}{m_2}}$, the damping ratio ($\xi_1 = \frac{c_1\omega_1}{2K_1}$) and the external excitation frequency (ω).

A typical shape of this function has been obtained for the configuration shown in figure 5.8. The values of the parameters do not match with the ones of the wing and the pod studied. There is no need for that in order to show the qualitative influence of the mass damper on the system.

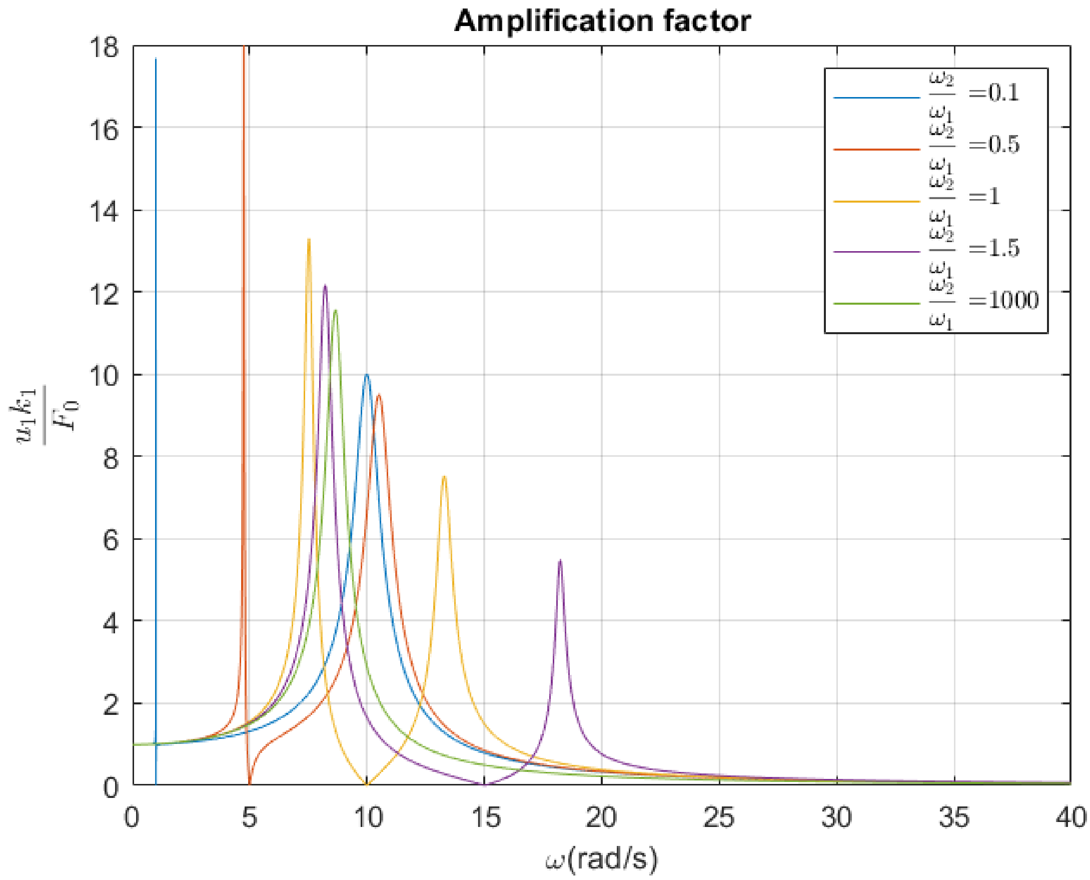

Figure 5.9: Amplification factor in a system with $\mu = \frac{1}{3}$, $\omega_1 = 10\frac{rad}{s}$ and $\xi_1 = 0.05$ for a range of ω_2 and ω

The figure shows that properly tuning the stiffness of the spring k_2 (i.e. its natural frequency ω_2), the values of ω where the function has a minimum or a maximum can be changed. The minimum amplification happens when the load acts near the natural frequency of the mass damper. This system proves to be very effective when the frequencies of the external loads are known.

Using pod and springs as mass dampers.

If the pod was considered as a combination of two mass dampers, a torsional and a longitudinal one, their resonance frequencies could be easily tuned in order to match the unknown external load frequency.

The resonance frequency of a longitudinal spring mass damper is $f = \frac{1}{2\pi}\sqrt{\frac{k_v}{m}}$, while for a torsion spring it is $f = \frac{1}{2\pi}\sqrt{\frac{k_\theta}{I}}$. Where m is its mass and I, its moment of inertia.

The pod mass and inertia values are $m_{pod} = 328.3kg$ and $I_{pod} = 161.7kgm^2$. Consequently, the desired values of stiffness to reduce vibrations would be $k_v = (2\pi f)^2 m_{pod}$ and $k_\theta = (2\pi f)^2 I_{pod}$, with f the frequency of the external load.

This criteria of selecting stiffness values will be applied in section (6.1) to increase the flutter-boundary velocity.

5.4 Analysis of the first plunge and torsion modes. Wing and pod motion decoupling

Another criteria to tune the stiffness constants is presented in this subsection.

In order to understand how stiffness will affect the shape of the first modes of plunge and torsion, a representation of the free-wing (stiffness constants equal to zero) and joined-wing (rigidly attached to the pod) is shown in Figure 5.10 and Figure 5.11.

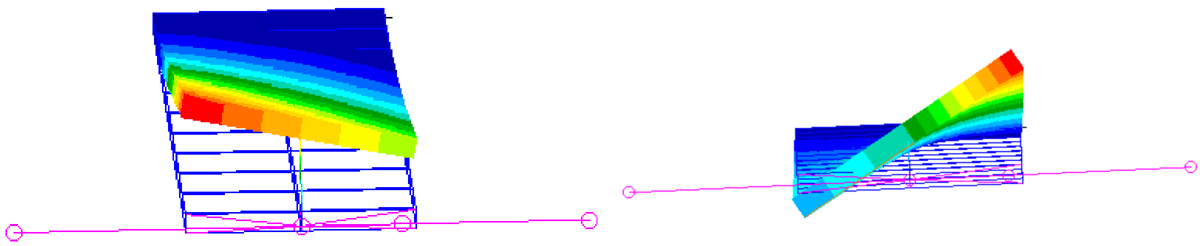

(a) Mode 1.
$f_1 = 1.77H_z$

(b) Mode 2.
$f_2 = 3.04H_z$

Figure 5.10: Free wing modes.

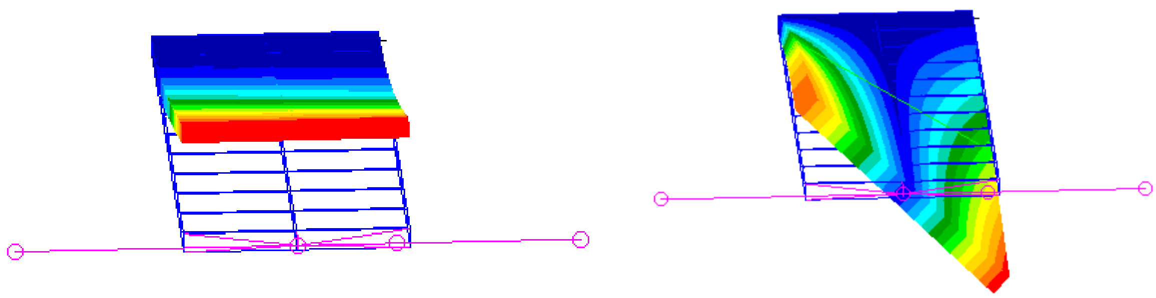

(a) Mode 1.
$f_1 = 1.58H_z$

(b) Mode 2.
$f_2 = 2.25H_z$

Figure 5.11: Rigid-joined wing modes.

Figure 5.10 shows that plunge and torsion are coupled for the first two modes of the free-wing. One design requirement could be to uncouple the first two modes of the wing so that there would be pure plunge for the first one and pure torsion for the second. To achieve this, their frequencies have to be close to the ones of the rigid joining case, which involves high values of stiffness.

Furthermore, an additional goal could be to uncouple the motion between wing and pod. This means that the vertical displacement and pitch of the pod would not be influenced by the plunge and torsion of the wing. This uncoupling condition can be achieved by maximizing the relative motion between pod and wing. And by recalling the results obtained in section 5.2.1, this relative motion was increased by setting low values of k_v and k_θ.

In conclusion, in order to satisfy both of the mentioned requirements a compromise solution must be achieved. By trying to find intermediate stiffness values, and using the results from Figure 5.4 and Figure 5.5, a couple of stiffness constants that satisfy the frequency constraint are $k_v = 3.75 \cdot 10^5 N/m$ and $k_\theta = 3.75 \cdot 10^5 Nm/rad$. It was proved that lower values of stiffness constants provided a first mode of pure plunge, but they degraded the response of the second mode, so they were discarded. The modal shapes using the selected stiffness constants are shown in Figure 5.12.

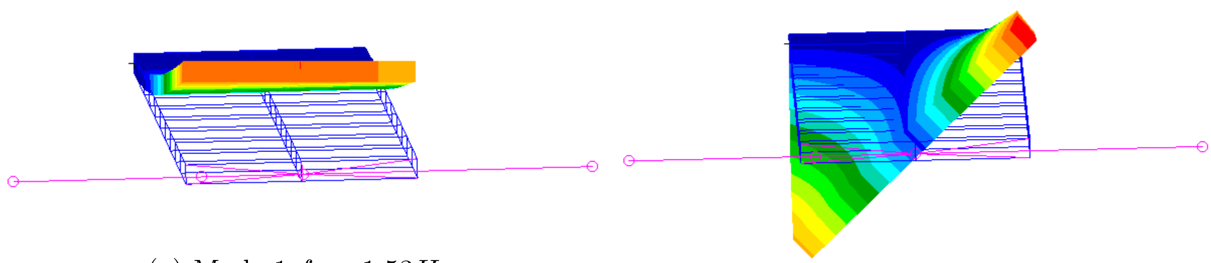

(a) Mode 1.$f_1 = 1.53H_z$

(b) Mode 2.$f_2 = 2.18H_z$

Figure 5.12: Natural modes of the wing-pod system

These results show that the rotation motion around the wing axis has been significantly damped in the first mode, resulting in a quasi-pure plunge mode. Additionally, the vertical displacement amplitude in the second mode has been reduced in contrast to the free-wing second mode. Regarding the natural frequencies, they are lower than the ones of the rigid joined wing (1.16% for first mode and 2.24% for the second one). Finally, the relative vibration amplitude between the wing's tip and the pod is $\frac{v_{pod}}{v_{wing}} = 1.0929$ in the first mode and $\frac{\theta_{pod}}{\theta_{wing}} = 1.0913$ in the second mode. This pair of stiffness constants provides a compromise solution for the mentioned requirements.

The influence of these results in $V_{EAS}|_{flutter}$ will be discussed in section 6.1.

Chapter 6

Flutter Instability in the Flexible Joint Configuration

Spring stiffness values alter the response of the wing to flutter instability, as they modify the natural behaviour of the structure to free vibration as well as its interaction with the aerodynamic forces.

It is important to recall from the flutter analysis in the rigid joining case that flutter occurred at $V_{EAS} = 65.8\frac{m}{s}$ for the first normal mode, while at $V_{EAS} = 93.9\frac{m}{s}$ the dynamic divergence appeared for the second one.

Spring stiffness can be tuned in order to increase the flutter-boundary speed. In this section, the results of two different procedures are shown. The first one, is based on the concept of mass dumper explained in section 5.3.1; the second one consists in uncoupling the torsion and flexion of the first two modes of the structure, explained in section 5.4. Each procedure returns two different values for k_v and k_θ, and a different value of flutter boundary velocity.

6.1 Increasing flutter speed matching flutter and mass damper resonance frequency

In section 5.3.1, the use of the pod as a mass damper was explained and it was said that it was possible to reduce the vibrations of the system by tuning its resonance frequency. This was very useful when the frequency of the external load acting on the structure was known. Following this idea, in order to increase the velocity of the flutter boundary, the resonance frequency of the mass damper should be close to the frequency where flutter instability is expected to appear.

In the rigid attachment configuration, flutter instability was associated with a frequency

$f_{flutter} = 1.61Hz$. The pod has a mass $m_{pod} = 328.3kg$. Therefore, in order to improve flutter, its stiffness should be $k_v = m_{pod}(2\pi f_{flutter})^2 = 3.36 \cdot 10^4 N/m$.

The torsional spring can be tuned in the same way. With $I_{pod} = 161kgm^2$, $k_\theta = I_{pod}(2\pi f_{flutter})^2 = 1.65 \cdot 10^4 Nm/rad$.

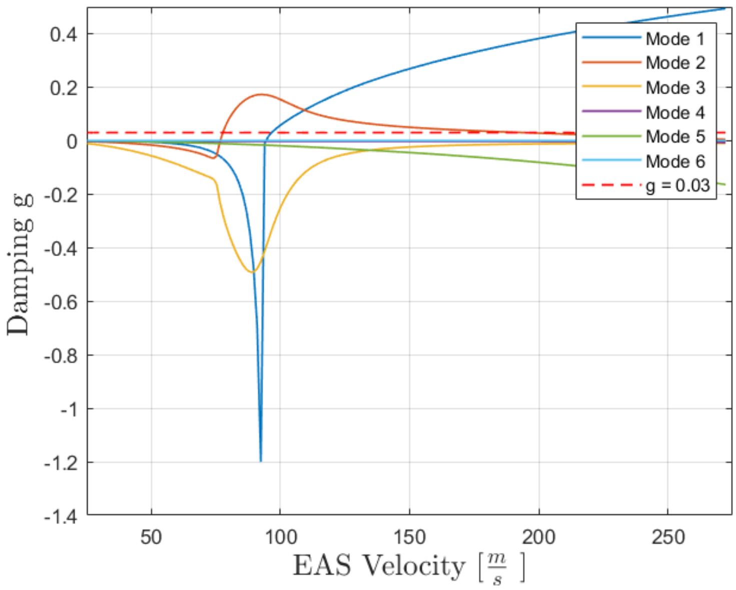

Figure 6.1: V-g Diagram with $k_v = 3.36 \cdot 10^4 N/m$ and $k_\theta = 1.65 \cdot 10^4 Nm/rad$

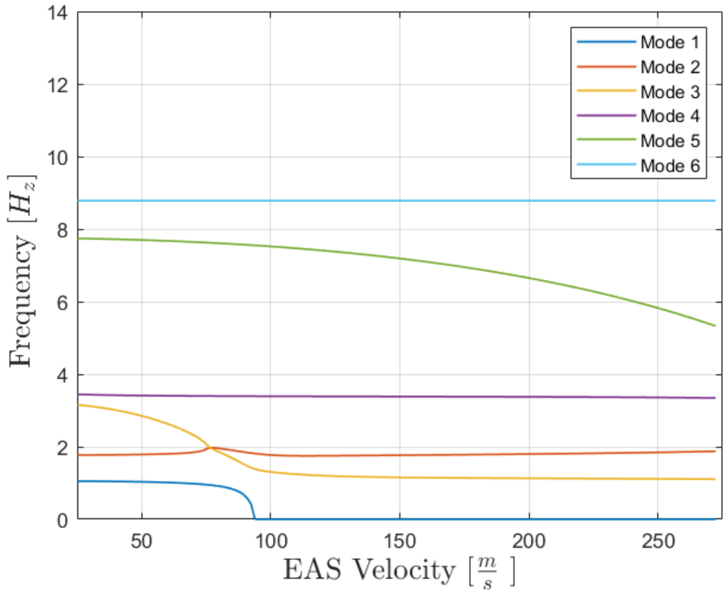

Figure 6.2: V-f Diagram with $k_v = 3.3610^4 \cdot N/m$ and $k_\theta = 1.65 \cdot 10^4 Nm/rad$

Figure 6.1 and 6.2 show that flutter is no longer associated with the first mode, but with the second one, at a velocity $V_{EAS} = 77.7\frac{m}{s}$, that is greater than in the rigid case and at a frequency $f_{flutter} = 2Hz$.

By tuning again the mass damper for the new flutter frequency: $k_v = 5.185 \cdot 10^4 N/m$ and $k_\theta = 2.542 \cdot 10^4 Nm/rad$.

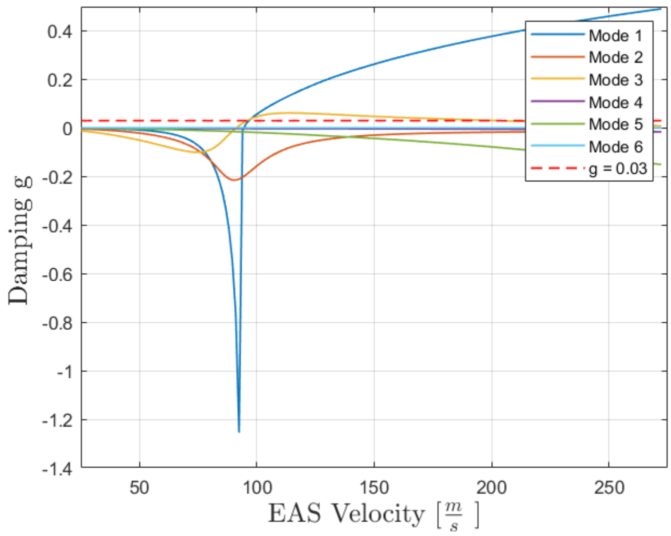

Figure 6.3: V-g Diagram with $k_v = 5.185 \cdot 10^4 N/m$ and $k_\theta = 2.542 \cdot 10^4 Nm/rad$

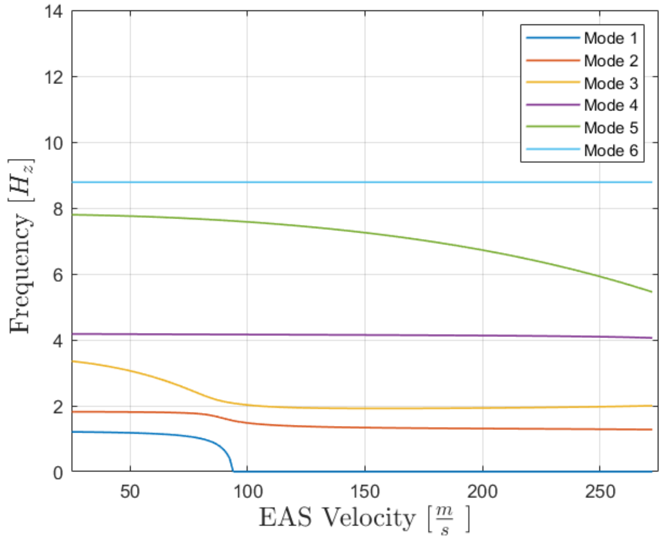

Figure 6.4: V-f Diagram with $k_v = 5.185 \cdot 10^4 N/m$ and $k_\theta = 2.542 \cdot 10^4 Nm/rad$

Flutter velocity has increased again. Now its value is $95.7\frac{m}{s}$, almost the same as the divergence velocity, which is not affected by the spring stiffness. The flutter frequency for this case is $2.1Hz$. Now flutter is associated with the third mode.

The third iteration is the last one, as it returns the same flutter frequency than the second one ($f = 2.1Hz$). The stiffness are $k_v = 5.716 \cdot 10^4 N/m$ and $k_\theta = 2.803 \cdot 10^4 Nm/rad$. Its diagrams are shown below:

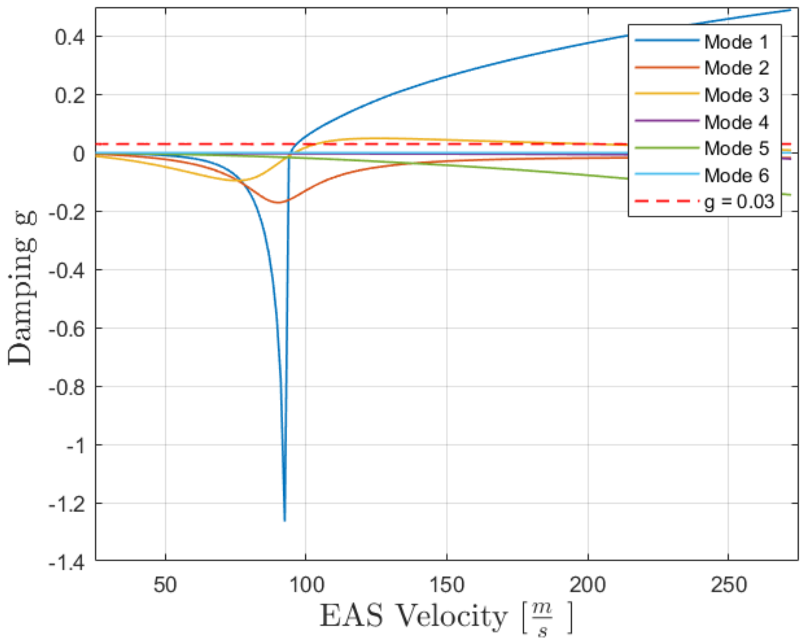

Figure 6.5: V-g Diagram with $k_v = 5.716 \cdot 10^4 N/m$ and $k_\theta = 2.803 \cdot 10^4 Nm/rad$

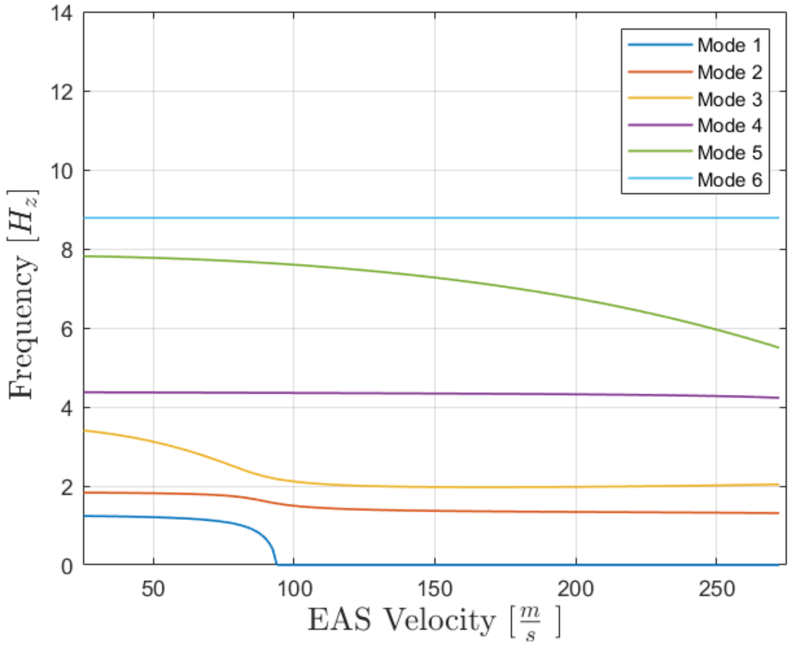

Figure 6.6: V-f Diagram with $k_v = 5.716 \cdot 10^4 N/m$ and $k_\theta = 2.803 \cdot 10^4 Nm/rad$

Flutter boundary appears at mode 3, at a velocity $V_{EAS} = 103\frac{m}{s}$.

This procedure to tune springs has shown good results to increase flutter velocity. The values of k_v and k_θ obtained are not the optimal ones for increasing it, as the relation between modes, frequencies and aerodynamic loading is complex and a more extended analysis would be necessary to find them. However they will be used as initial points for a sensitivity analysis of flutter-speed boundary.

As a general rule, the improvement the flutter is associated to the separation in frecuency of the modes that exchange energy between them, as it can be seen in the previous graphs.

6.1.1 Frequency analysis

A frequency analysis has been carried out for the rigid joint configuration and for the wing with the values of stiffness obtained at the end of section 6.1 ($k_v = 5.716 \cdot 10^4 N/m$ and $k_\theta = 2.803 \cdot 10^4 Nm/rad$). The results obtained are the displacement of the external wing rib (grid 20005) when a load of frequency f is applied on that same node. SOL 111 of Nastran has been used for this purpose. Figure 6.7 shows how different the dynamic behaviour of both configurations is.

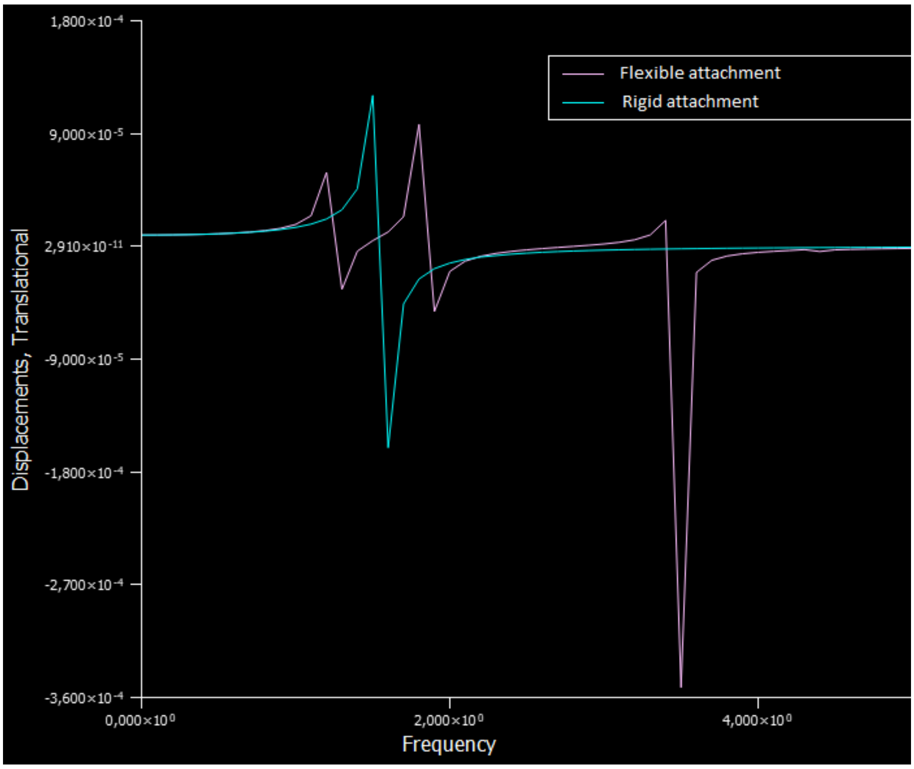

Figure 6.7: Relation between vertical displacement and frequency for the vertical load applied.

6.2 Influence of decoupling modes on flutter phenomena

In section 5.4, a pair of spring stiffness values were obtained following a criteria of decoupling torsional and plunge modes. In this section, it will be shown how the results of applying the PKNL method in Nastran with those stiffness ($k_v = 3.75 \cdot 10^5 \frac{N}{m}$ and $K_\theta = 3.75 \cdot 10^5 \frac{Nm}{rad}$) will have an influence on flutter phenomenon.

The Figure 6.8 showing the damping coefficient confirms a static divergence at the same point where the rigid-joined model also diverges, while flutter disappears completely.

Furthermore, it can be seen in Figures 6.8 and 6.9 how the second mode (red curve) tries to get into flutter by extracting energy from the first (blue curve) and third mode (yellow curve), which slowly decreases its damping and frequency. In the end, the frequencies of both modes 2 and 3 get to be separated from each other, which means that mode 2 does not get to extract the sufficient energy from mode 3 to get over the 3% damping line.

As a conclusion, it can be noticed that both springs not only manage to uncouple the normal modes but they also increase the flutter speed to an undefined limit.

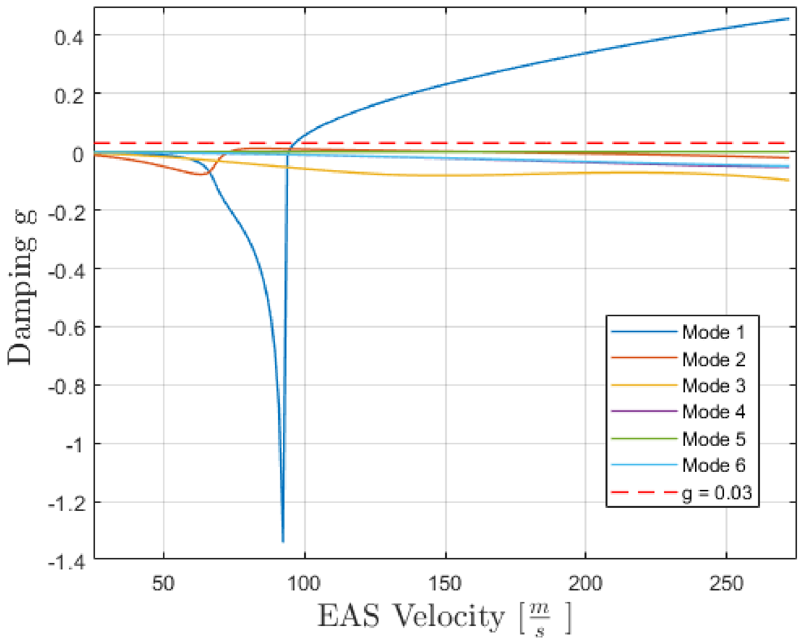

Figure 6.8: V-g diagram with the implemented springs

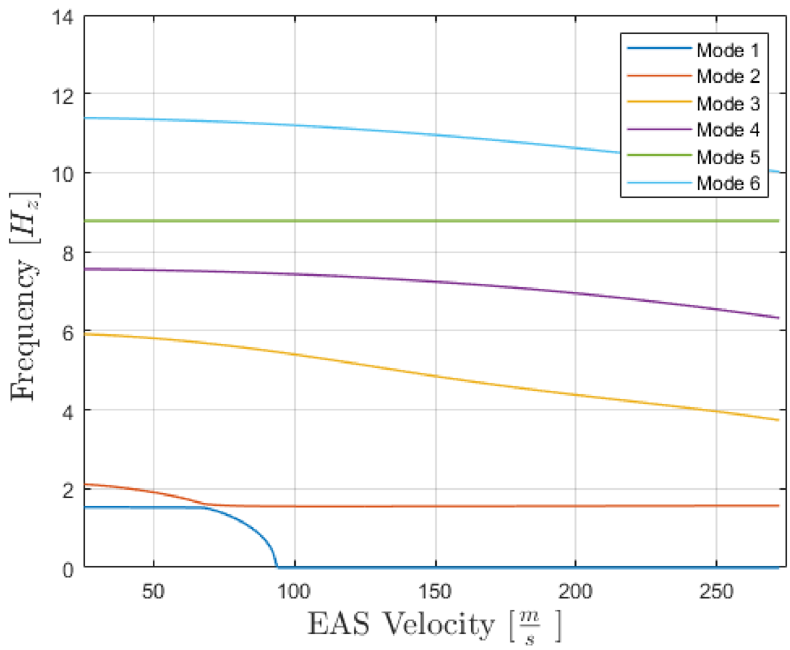

Figure 6.9: V-f diagram with the implemented springs

6.3 Chosen spring stiffness values

In the previous sections 6.1 and 6.2, stability boundaries for two different pairs of spring stiffness were studied. The pair obtained in section 6.1 increases flutter velocity by 56%, which is a significant improvement in terms of stability. The other pair, obtained in 5.4, has shown an even better improvement, as flutter does not occur for the studied flight conditions. Therefore, these last ones will be chosen as the final values for the flexible joint that will satisfy the mentioned design requirements ($k_v = 3.75 \cdot 10^5 N/m$ and $k_\theta = 3.75 \cdot 10^5 Nm/rad$).

Chapter 7

Sensitivity Analysis

It has been proved from section 6.2 that there were values of k_v and k_θ for which not only could the first normal modes of the wing be uncoupled but they also managed to avoid flutter at $M = 0.8$.

However, if these stiffness values were to be used as the central points within a range of k_v and k_θ to find how flutter velocities vary in a sensitivity analysis, the latter could not be performed since flutter does not appear as mentioned above.

Indeed, for this sensitivity analysis, the pair of k_v and k_θ that have been used are the ones obtained in section 6.1, in which the concept of *mass damper* was used in order to find stiffness values that would progressively increase the flutter-boundary velocity. These values are: $k_v = 5.716 \cdot 10^4 \frac{N}{m}$ and $k_\theta = 2.803 \frac{Nm}{rad}$

The analysis was set up to express flutter speed as a function of the torsion spring constant, k_θ, in which k_v remained as variable parameter. By running several simulations the results obtained are shown in figure 7.1.

Notice how flutter speed always grows with both spring constants in the range selected.

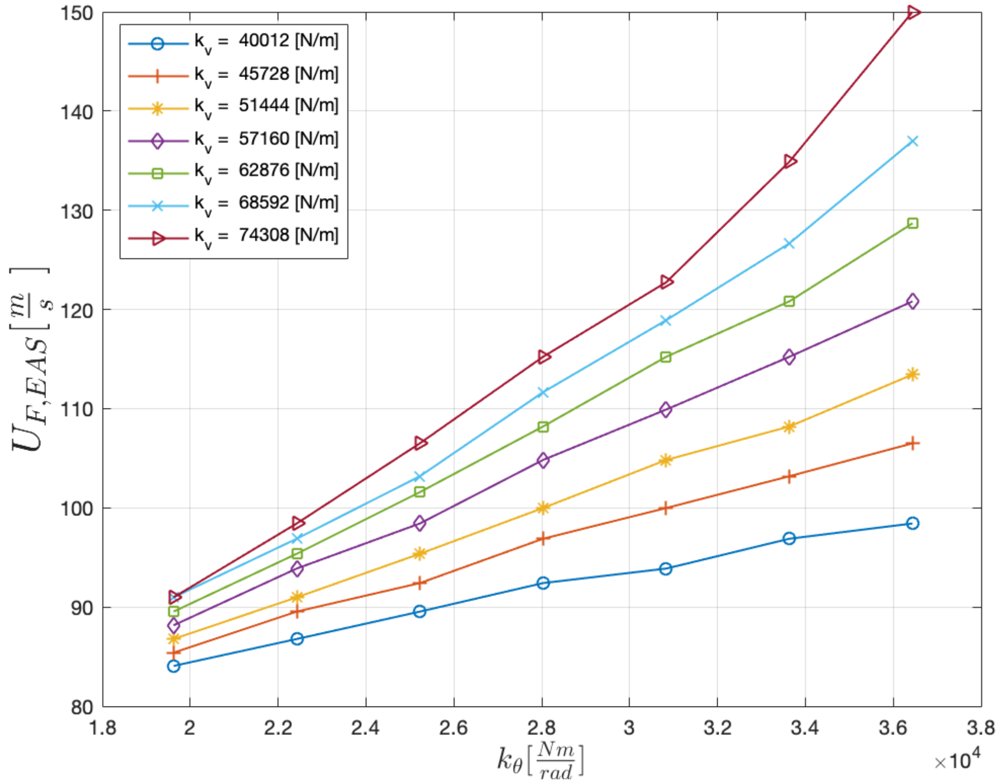

Figure 7.1: Evolution of flutter-boundary speed as a function of k_v, for different constant values of k_θ

Increasing stiffness along the gradient direction might result in obtaining an optimal pair of values. There is no need to do that, as a pair of stiffness values that avoid flutter has already been obtained. Nevertheless, this figure shows valuable information, as for example, how sensitive flutter velocity $U_{F,EAS}$ is to changes in stiffness.

However, the behaviour of the system is not monotonous as it can be expected with figure 7.1. When high enough values are reached, the flutter velocity decreases again. This fact is proved because when both k tend to infinite (rigid case), the flutter velocity tends to $65.8m/s$.

Chapter 8

Concluding Remarks

The present work has accomplished all its objectives. Firstly, the structure has been characterized by its first 16 normal modes (the ones with a frecuency below $50Hz$). In addition, its generalized mass and stiffness matrices have been calculated.

After describing the flutter equation for the K-Method, a flutter analysis with Nastran has been carried out, using the PK method. As a result, the instability boundaries of the wing (flutter and divergence) have been obtained. There was a big difference between the flutter-boundary velocity and divergence velocity. The range of operation is limited by the lowest of these two (flutter in this case).

The suggested structural alteration of the wing, which consisted in changing the rigid joint between wing and pod into a flexible one, was successfully implemented in the model. The stiffness values of the springs used in the flexible union were used as design variables in order to reduce wing vibrations.

An initial requirement of design was to reduce pod vibrations related to those of the wing. However, this report proved that it was not possible. The configuration under which they are minimum is the rigid case.

Nevertheless, wing vibrations could be reduced by properly tuning the spring stiffness based on the *mass damper* concept. By doing so, flutter-instability velocity could be increased.

A second requirement was to uncouple motion between wing and pod, which has also been achieved.

All together, two different approaches were made in order to correctly set the spring stiffness. Both have shown very good results; the first one increased flutter velocity by 56%, while the other makes flutter to disappear.

Hence, the modified wing range of operation is no longer limited by flutter, as the most restrictive speed is the one for which divergence appears, on which flexible joining has no effect. If the design goal was to increase this range, the divergence speed should be increased.

A way to do this without altering the structure, is by choosing a material with an higher Young's module. The ultimate configuration will be able to fly at higher speeds and lower altitudes than the initial one. These changes could make the wing more valuable to potential customers as it could be used in a more extended flight envelope, turning it into a more versatile wing.

Chapter 9

Appendix

9.1 Bdf file for flutter analysis of rigid joint configuration

```
$ ======================================================================
$                      SOL 145 - flutter Analysis
$ ======================================================================
$
$ ------------------   File Management Section   -----------------------
$ ASSIGN OUTPUT4 = 'btb.f50',UNIT = 50,FORM=FORMATTED
$
$ ------------------   Executive Control Deck   -----------------------
$
ID                  MSC.NASTRAN FLUTTER ANALYSIS
SOL                 145    ← Flutter Solution
TIME                5000
$
$ ------------------   Executive Control Deck   -----------------------
$
CEND
$
$ ------------------   Case Control Deck   -----------------------------
$
TITLE               = FLUTTER ANALYSIS
SUBTITLE            = (SOL145)
$
ECHO                = NONE
SEALL               = ALL
SPC                 = 999
METHOD              = 200    ← Real Eigenvalue Method Selection
FMETHOD             = 300    ← Flutter Analysis Method Selection
RESVEC              = NO
DISPLACEMENT        = ALL
$
$...1...|...2...|...3...|...4...|...5...|...6...|...7...|...8...|...9...|..10...
PARAM   POST    0
PARAM   GRDPNT  0
PARAM   OPPHIPA 1
PARAM   PRTMAXIM YES
PARAM   OPPHIB   1

BEGIN BULK
$ MATERIAL QUE USA PARA LAS BARRAS(PROD) Y PARA LAS CHAPAS O REVESTIMIENTO (PSHELL)
$...1...|...2...|...3...|...4...|...5...|...6...|...7...|...8...|...9...|..10...
MAT1    1       7.171+102.689+10        5.1538-4
$
$ GRIDS DEL LA LINEA MORADA DE LA RAIZ DEL ALA:POD
GRID     20001          0.6096  6.2484 0.               123456
GRID     20002          0.0762  6.2484 0.
GRID     20003          -0.9144 6.2484 0.
GRID     20004          2.1336  6.2484 0.
$ CREO LAS LINEAS MORADAS: BARRAS RIGIDAS
RBAR    3001    20001   20002   123456
RBAR    3002    20002   20003   123456
RBAR    3003    20001   20004   123456
$


$ GRIDS QUE FORMAN EL ALA, A PARTIR DE LOS CUALES SE DEFINEN LOS CROD Y CQUAD4
```

```
GRID     10204           0.6096  1.2192 -.0508
GRID     10205           1.2192  1.2192 -.0508
GRID     10300           0.      1.8288  .0508
GRID     10301           0.6096  1.8288  .0508
GRID     10302           1.2192  1.8288  .0508
GRID     10303           0.      1.8288 -.0508
GRID     10304           0.6096  1.8288 -.0508
GRID     10305           1.2192  1.8288 -.0508
GRID     10400           0.      2.4384  .0508
GRID     10401           0.6096  2.4384  .0508
GRID     10402           1.2192  2.4384  .0508
GRID     10403           0.      2.4384 -.0508
GRID     10404           0.6096  2.4384 -.0508
GRID     10405           1.2192  2.4384 -.0508
GRID     10500           0.      3.048   .0508
GRID     10501           0.6096  3.048   .0508
GRID     10502           1.2192  3.048   .0508
GRID     10503           0.      3.048  -.0508
GRID     10504           0.6096  3.048  -.0508
GRID     10505           1.2192  3.048  -.0508
GRID     10600           0.      3.6576  .0508
GRID     10601           0.6096  3.6576  .0508
GRID     10602           1.2192  3.6576  .0508
GRID     10603           0.      3.6576 -.0508
GRID     10604           0.6096  3.6576 -.0508
GRID     10605           1.2192  3.6576 -.0508
GRID     10700           0.      4.2672  .0508
GRID     10701           0.6096  4.2672  .0508
GRID     10702           1.2192  4.2672  .0508
GRID     10703           0.      4.2672 -.0508
GRID     10704           0.6096  4.2672 -.0508
GRID     10705           1.2192  4.2672 -.0508
GRID     10800           0.      4.8768  .0508
GRID     10801           0.6096  4.8768  .0508
GRID     10802           1.2192  4.8768  .0508
GRID     10803           0.      4.8768 -.0508
GRID     10804           0.6096  4.8768 -.0508
GRID     10805           1.2192  4.8768 -.0508
GRID     10900           0.      5.4864  .0508
GRID     10901           0.6096  5.4864  .0508
GRID     10902           1.2192  5.4864  .0508
GRID     10903           0.      5.4864 -.0508
GRID     10904           0.6096  5.4864 -.0508
GRID     10905           1.2192  5.4864 -.0508
GRID     11000           0.      6.096   .0508
GRID     11001           0.6096  6.096   .0508
GRID     11002           1.2192  6.096   .0508
GRID     11003           0.      6.096  -.0508
GRID     11004           0.6096  6.096  -.0508
GRID     11005           1.2192  6.096  -.0508
$
GRID     12000           1.8288  0.      .0508
SPC1     999     123456  12000


$...1...|...2...|...3...|...4...|...5...|...6...|...7...|...8...|...9...|..10...
SPC          999   10000       1
SPC          999   10000       2
SPC          999   10000       3
SPC          999   10000       4
SPC          999   10000       5
SPC          999   10000       6
SPC          999   10001       1
SPC          999   10001       2
SPC          999   10001       3
SPC          999   10001       4
SPC          999   10001       5
SPC          999   10001       6
SPC          999   10002       1
SPC          999   10002       2
SPC          999   10002       3
SPC          999   10002       4
```

```
SPC           999   10002       5
SPC           999   10002       6
SPC           999   10003       1
SPC           999   10003       2
SPC           999   10003       3
SPC           999   10003       4
SPC           999   10003       5
SPC           999   10003       6
SPC           999   10004       1
SPC           999   10004       2
SPC           999   10004       3
SPC           999   10004       4
SPC           999   10004       5
SPC           999   10004       6
SPC           999   10005       1
SPC           999   10005       2
SPC           999   10005       3
SPC           999   10005       4
SPC           999   10005       5
SPC           999   10005       6
SPC           999   10100       4
SPC           999   10100       5
SPC           999   10100       6
SPC           999   10101       4
SPC           999   10101       5
SPC           999   10101       6
SPC           999   10102       4
SPC           999   10102       5
SPC           999   10102       6
SPC           999   10103       4
SPC           999   10103       5
SPC           999   10103       6
SPC           999   10104       4
SPC           999   10104       5
SPC           999   10104       6
SPC           999   10105       4
SPC           999   10105       5
SPC           999   10105       6
SPC           999   10200       4
SPC           999   10200       5
SPC           999   10200       6
SPC           999   10201       4
SPC           999   10201       5
SPC           999   10201       6
SPC           999   10202       4
SPC           999   10202       5
SPC           999   10202       6
SPC           999   10203       4
SPC           999   10203       5
SPC           999   10203       6
SPC           999   10204       4
SPC           999   10204       5
SPC           999   10204       6
SPC           999   10205       4
SPC           999   10205       5
SPC           999   10205       6
SPC           999   10300       4
SPC           999   10300       5
SPC           999   10300       6
SPC           999   10301       4
SPC           999   10301       5
SPC           999   10301       6
SPC           999   10302       4
SPC           999   10302       5
SPC           999   10302       6
SPC           999   10303       4
SPC           999   10303       5
SPC           999   10303       6
SPC           999   10304       4
SPC           999   10304       5
SPC           999   10304       6
SPC           999   10305       4
```

```
SPC            999   10305        5
SPC            999   10305        6
SPC            999   10400        4
SPC            999   10400        5
SPC            999   10400        6
SPC            999   10401        4
SPC            999   10401        5
SPC            999   10401        6
SPC            999   10402        4
SPC            999   10402        5
SPC            999   10402        6
SPC            999   10403        4
SPC            999   10403        5
SPC            999   10403        6
SPC            999   10404        4
SPC            999   10404        5
SPC            999   10404        6
SPC            999   10405        4
SPC            999   10405        5
SPC            999   10405        6
SPC            999   10500        4
SPC            999   10500        5
SPC            999   10500        6
SPC            999   10501        4
SPC            999   10501        5
SPC            999   10501        6
SPC            999   10502        4
SPC            999   10502        5
SPC            999   10502        6
SPC            999   10503        4
SPC            999   10503        5
SPC            999   10503        6
SPC            999   10504        4
SPC            999   10504        5
SPC            999   10504        6
SPC            999   10505        4
SPC            999   10505        5
SPC            999   10505        6
SPC            999   10600        4
SPC            999   10600        5
SPC            999   10600        6
SPC            999   10601        4
SPC            999   10601        5
SPC            999   10601        6
SPC            999   10602        4
SPC            999   10602        5
SPC            999   10602        6
SPC            999   10603        4
SPC            999   10603        5
SPC            999   10603        6
SPC            999   10604        4
SPC            999   10604        5
SPC            999   10604        6
SPC            999   10605        4
SPC            999   10605        5
SPC            999   10605        6
SPC            999   10700        4
SPC            999   10700        5
SPC            999   10700        6
SPC            999   10701        4
SPC            999   10701        5
SPC            999   10701        6
SPC            999   10702        4
SPC            999   10702        5
SPC            999   10702        6
SPC            999   10703        4
SPC            999   10703        5
SPC            999   10703        6
SPC            999   10704        4
SPC            999   10704        5
SPC            999   10704        6
SPC            999   10705        4
```

```
SPC          999   10705       5
SPC          999   10705       6
SPC          999   10800       4
SPC          999   10800       5
SPC          999   10800       6
SPC          999   10801       4
SPC          999   10801       5
SPC          999   10801       6
SPC          999   10802       4
SPC          999   10802       5
SPC          999   10802       6
SPC          999   10803       4
SPC          999   10803       5
SPC          999   10803       6
SPC          999   10804       4
SPC          999   10804       5
SPC          999   10804       6
SPC          999   10805       4
SPC          999   10805       5
SPC          999   10805       6
SPC          999   10900       4
SPC          999   10900       5
SPC          999   10900       6
SPC          999   10901       4
SPC          999   10901       5
SPC          999   10901       6
SPC          999   10902       4
SPC          999   10902       5
SPC          999   10902       6
SPC          999   10903       4
SPC          999   10903       5
SPC          999   10903       6
SPC          999   10904       4
SPC          999   10904       5
SPC          999   10904       6
SPC          999   10905       4
SPC          999   10905       5
SPC          999   10905       6
SPC          999   11000       4
SPC          999   11000       5
SPC          999   11000       6
SPC          999   11001       4
SPC          999   11001       5
SPC          999   11001       6
SPC          999   11002       4
SPC          999   11002       5
SPC          999   11002       6
SPC          999   11003       4
SPC          999   11003       5
SPC          999   11003       6
SPC          999   11004       4
SPC          999   11004       5
SPC          999   11004       6
SPC          999   11005       4
SPC          999   11005       5
SPC          999   11005       6


$...1...|...2...|...3...|...4...|...5...|...6...|...7...|...8...|...9...|..10...
RBE3    2100           20001   123456  1.0     123     11000   11001   +6001
+6001   11002   11003   11004   11005

$...1...|...2...|...3...|...4...|...5...|...6...|...7...|...8...|...9...|..10...
PROD     5       1      2.5000-5
$
CROD     100     5       10003   10000
CROD     101     5       10004   10001
CROD     102     5       10005   10002
CROD     103     5       10103   10100
CROD     104     5       10104   10101
CROD     105     5       10105   10102
CROD     106     5       10203   10200
```

```
CROD    107     5       10204   10201
CROD    108     5       10205   10202
CROD    109     5       10303   10300
CROD    110     5       10304   10301
CROD    111     5       10305   10302
CROD    112     5       10403   10400
CROD    113     5       10404   10401
CROD    114     5       10405   10402
CROD    115     5       10503   10500
CROD    116     5       10504   10501
CROD    117     5       10505   10502
CROD    118     5       10603   10600
CROD    119     5       10604   10601
CROD    120     5       10605   10602
CROD    121     5       10703   10700
CROD    122     5       10704   10701
CROD    123     5       10705   10702
CROD    124     5       10803   10800
CROD    125     5       10804   10801
CROD    126     5       10805   10802
CROD    127     5       10903   10900
CROD    128     5       10904   10901
CROD    129     5       10905   10902
CROD    130     5       11003   11000
CROD    131     5       11004   11001
CROD    132     5       11005   11002
$
$...1...|...2...|...3...|...4...|...5...|...6...|...7...|...8...|...9...|..10...
PROD    6       1      2.5000-3
$
CROD    133     6       10000   10001
CROD    134     6       10001   10002
CROD    135     6       10003   10004
CROD    136     6       10004   10005
CROD    137     6       10100   10101
CROD    138     6       10101   10102
CROD    139     6       10103   10104
CROD    140     6       10104   10105
CROD    141     6       10200   10201
CROD    142     6       10201   10202
CROD    143     6       10203   10204
CROD    144     6       10204   10205
CROD    145     6       10300   10301
CROD    146     6       10301   10302
CROD    147     6       10303   10304
CROD    148     6       10304   10305
CROD    149     6       10400   10401
CROD    150     6       10401   10402
CROD    151     6       10403   10404
CROD    152     6       10404   10405
CROD    153     6       10500   10501
CROD    154     6       10500   10502
CROD    155     6       10503   10504
CROD    156     6       10504   10505
CROD    157     6       10600   10601
CROD    158     6       10601   10602
CROD    159     6       10603   10604
CROD    160     6       10604   10605
CROD    161     6       10700   10701
CROD    162     6       10701   10702
CROD    163     6       10703   10704
CROD    164     6       10704   10705
CROD    165     6       10800   10801
CROD    166     6       10801   10802
CROD    167     6       10803   10804
CROD    168     6       10804   10805
CROD    169     6       10900   10901
CROD    170     6       10901   10902
CROD    171     6       10903   10904
CROD    172     6       10905   10904
CROD    173     6       11000   11001
CROD    174     6       11001   11002
```

```
CROD    175     6       11003   11004
CROD    176     6       11004   11005
$
$...1...|...2...|...3...|...4...|...5...|...6...|...7...|...8...|...9...|..10...
PROD    7       1      2.5000-3
$
CROD    177     7       10000   10100
CROD    178     7       10003   10103
CROD    179     7       10100   10200
CROD    180     7       10103   10203
CROD    181     7       10200   10300
CROD    182     7       10203   10303
CROD    183     7       10300   10400
CROD    184     7       10303   10403
CROD    185     7       10400   10500
CROD    186     7       10403   10503
CROD    187     7       10500   10600
CROD    188     7       10503   10603
CROD    189     7       10600   10700
CROD    190     7       10603   10703
CROD    191     7       10700   10800
CROD    192     7       10703   10803
CROD    193     7       10800   10900
CROD    194     7       10803   10903
CROD    195     7       10900   11000
CROD    196     7       10903   11003
CROD    197     7       10002   10102
CROD    198     7       10005   10105
CROD    199     7       10102   10202
CROD    200     7       10105   10205
CROD    201     7       10202   10302
CROD    202     7       10205   10305
CROD    203     7       10302   10402
CROD    204     7       10305   10405
CROD    205     7       10402   10502
CROD    206     7       10405   10505
CROD    207     7       10502   10602
CROD    208     7       10505   10605
CROD    209     7       10602   10702
CROD    210     7       10605   10705
CROD    211     7       10702   10802
CROD    212     7       10705   10805
CROD    213     7       10802   10902
CROD    214     7       10805   10905
CROD    215     7       10902   11002
CROD    216     7       10905   11005
$
$...1...|...2...|...3...|...4...|...5...|...6...|...7...|...8...|...9...|..10...
PROD    8       1      1.5000-2
$
CROD    217     8       10001   10101
CROD    218     8       10004   10104
CROD    219     8       10101   10201
CROD    220     8       10104   10204
CROD    221     8       10201   10301
CROD    222     8       10204   10304
CROD    223     8       10301   10401
CROD    224     8       10304   10404
CROD    225     8       10401   10501
CROD    226     8       10404   10504
CROD    227     8       10501   10601
CROD    228     8       10504   10604
CROD    229     8       10601   10701
CROD    230     8       10604   10704
CROD    231     8       10701   10801
CROD    232     8       10704   10804
CROD    233     8       10801   10901
CROD    234     8       10804   10904
CROD    235     8       10901   11001
CROD    236     8       10904   11004
$
$...1...|...2...|...3...|...4...|...5...|...6...|...7...|...8...|...9...|..10...
```

```
$ DEFINE EL ESPESOR DE LA CHAPA 0.0025
PSHELL   1       1      .0025000
$
CQUAD4   1       1       10000   10001   10101   10100
CQUAD4   2       1       10001   10002   10102   10101
CQUAD4   3       1       10100   10101   10201   10200
CQUAD4   4       1       10101   10102   10202   10201
CQUAD4   5       1       10200   10201   10301   10300
CQUAD4   6       1       10201   10202   10302   10301
CQUAD4   7       1       10300   10301   10401   10400
CQUAD4   8       1       10301   10302   10402   10401
CQUAD4   9       1       10400   10401   10501   10500
CQUAD4   10      1       10401   10402   10502   10501
CQUAD4   11      1       10500   10501   10601   10600
CQUAD4   12      1       10501   10502   10602   10601
CQUAD4   13      1       10600   10601   10701   10700
CQUAD4   14      1       10601   10602   10702   10701
CQUAD4   15      1       10700   10701   10801   10800
CQUAD4   16      1       10701   10702   10802   10801
CQUAD4   17      1       10800   10801   10901   10900
CQUAD4   18      1       10801   10802   10902   10901
CQUAD4   19      1       10900   10901   11001   11000
CQUAD4   20      1       10901   10902   11002   11001
CQUAD4   21      1       10003   10004   10104   10103
CQUAD4   22      1       10004   10005   10105   10104
CQUAD4   23      1       10103   10104   10204   10203
CQUAD4   24      1       10104   10105   10205   10204
CQUAD4   25      1       10203   10204   10304   10303
CQUAD4   26      1       10204   10205   10305   10304
CQUAD4   27      1       10303   10304   10404   10403
CQUAD4   28      1       10304   10305   10405   10404
CQUAD4   29      1       10403   10404   10504   10503
CQUAD4   30      1       10404   10405   10505   10504
CQUAD4   31      1       10503   10504   10604   10603
CQUAD4   32      1       10504   10505   10605   10604
CQUAD4   33      1       10603   10604   10704   10703
CQUAD4   34      1       10604   10605   10705   10704
CQUAD4   35      1       10703   10704   10804   10803
CQUAD4   36      1       10704   10705   10805   10804
CQUAD4   37      1       10803   10804   10904   10903
CQUAD4   38      1       10804   10805   10905   10904
CQUAD4   39      1       10903   10904   11004   11003
CQUAD4   40      1       10904   10905   11005   11004
$
$...1...|...2...|...3...|...4...|...5...|...6...|...7...|...8...|...9...|..10...
PSHELL   2       1      1.0000-4
$
CQUAD4   41      2       10003   10000   10100   10103
CQUAD4   42      2       10103   10100   10200   10203
CQUAD4   43      2       10203   10200   10300   10303
CQUAD4   44      2       10300   10400   10403   10303
CQUAD4   45      2       10400   10500   10503   10403
CQUAD4   46      2       10500   10600   10603   10503
CQUAD4   47      2       10600   10700   10703   10603
CQUAD4   48      2       10700   10800   10803   10703
CQUAD4   49      2       10800   10900   10903   10803
CQUAD4   50      2       10900   11000   11003   10903
CQUAD4   51      2       10002   10102   10105   10005
CQUAD4   52      2       10102   10202   10205   10105
CQUAD4   53      2       10202   10302   10305   10205
CQUAD4   54      2       10302   10402   10405   10305
CQUAD4   55      2       10402   10502   10505   10405
CQUAD4   56      2       10502   10602   10605   10505
CQUAD4   57      2       10602   10702   10705   10605
CQUAD4   58      2       10702   10802   10805   10705
CQUAD4   59      2       10802   10902   10905   10805
CQUAD4   60      2       10902   11002   11005   10905
$
$...1...|...2...|...3...|...4...|...5...|...6...|...7...|...8...|...9...|..10...
PSHELL   3       1      .017500
$
CQUAD4   61      3       10004   10001   10101   10104
```

```
CQUAD4  62      3       10104   10101   10201   10204
CQUAD4  63      3       10204   10201   10301   10304
CQUAD4  64      3       10304   10301   10401   10404
CQUAD4  65      3       10404   10401   10501   10504
CQUAD4  66      3       10504   10501   10601   10604
CQUAD4  67      3       10604   10601   10701   10704
CQUAD4  68      3       10704   10701   10801   10804
CQUAD4  69      3       10804   10801   10901   10904
CQUAD4  70      3       10904   10901   11001   11004
$
$...1...|...2...|...3...|...4...|...5...|...6...|...7...|...8...|...9...|..10...
PSHELL  4       1      .017500
$
CQUAD4  71      4       10003   10000   10001   10004
CQUAD4  72      4       10004   10001   10002   10005
CQUAD4  73      4       10103   10100   10101   10104
CQUAD4  74      4       10104   10101   10102   10105
CQUAD4  75      4       10203   10200   10201   10204
CQUAD4  76      4       10204   10201   10202   10205
CQUAD4  77      4       10303   10300   10301   10304
CQUAD4  78      4       10304   10301   10302   10305
CQUAD4  79      4       10403   10400   10401   10404
CQUAD4  80      4       10404   10401   10402   10405
CQUAD4  81      4       10503   10500   10501   10504
CQUAD4  82      4       10504   10501   10502   10505
CQUAD4  83      4       10603   10600   10601   10604
CQUAD4  84      4       10604   10601   10602   10605
CQUAD4  85      4       10703   10700   10701   10704
CQUAD4  86      4       10704   10701   10702   10705
CQUAD4  87      4       10803   10800   10801   10804
CQUAD4  88      4       10804   10801   10802   10805
CQUAD4  89      4       10903   10900   10901   10904
CQUAD4  90      4       10904   10901   10902   10905
CQUAD4  91      4       11003   11000   11001   11004
CQUAD4  92      4       11004   11001   11002   11005

$
$...1...|...2...|...3...|...4...|...5...|...6...|...7...|...8...|...9...|..10...
$ MASAS PUNTUALES DEL BORDE DE ATAQUE DEL ALA
CONM2   1000    10000           14.33851
CONM2   1001    10003           14.33851
CONM2   1002    10100           28.67702
CONM2   1003    10103           28.67702
CONM2   1004    10200           28.67702
CONM2   1005    10203           28.67702
CONM2   1006    10300           28.67702
CONM2   1007    10303           28.67702
CONM2   1008    10400           28.67702
CONM2   1009    10403           28.67702
CONM2   1010    10500           28.67702
CONM2   1011    10503           28.67702
CONM2   1012    10600           28.67702
CONM2   1013    10603           28.67702
CONM2   1014    10700           28.67702
CONM2   1015    10703           28.67702
CONM2   1016    10800           28.67702
CONM2   1017    10803           28.67702
CONM2   1018    10900           28.67702
CONM2   1019    10903           28.67702
CONM2   1020    11000           14.33851
CONM2   1021    11003           14.33851
$ MASAS PUNTUALES DEL EJE MEDIO DEL ALA
CONM2   1100    10001           28.78064
CONM2   1101    10004           28.78064
CONM2   1102    10101           57.56127
CONM2   1103    10104           57.56127
CONM2   1104    10201           57.56127
CONM2   1105    10204           57.56127
CONM2   1106    10301           57.56127
CONM2   1107    10304           57.56127
CONM2   1108    10401           57.56127
CONM2   1109    10404           57.56127
```

```
CONM2   1110    10501           57.56127
CONM2   1111    10504           57.56127
CONM2   1112    10601           57.56127
CONM2   1113    10604           57.56127
CONM2   1114    10701           57.56127
CONM2   1115    10704           57.56127
CONM2   1116    10801           57.56127
CONM2   1117    10804           57.56127
CONM2   1118    10901           57.56127
CONM2   1119    10904           57.56127
CONM2   1120    11001           28.78064
CONM2   1121    11004           28.78064
$ MASAS PUNTUALES DEL BORDE DE SALIDA DEL ALA
CONM2   1200    10002           38.96426
CONM2   1201    10005           38.96426
CONM2   1202    10102           77.92852
CONM2   1203    10105           77.92852
CONM2   1204    10202           77.92852
CONM2   1205    10205           77.92852
CONM2   1206    10302           77.92852
CONM2   1207    10305           77.92852
CONM2   1208    10402           77.92852
CONM2   1209    10405           77.92852
CONM2   1210    10502           77.92852
CONM2   1211    10505           77.92852
CONM2   1212    10602           77.92852
CONM2   1213    10605           77.92852
CONM2   1214    10702           77.92852
CONM2   1215    10705           77.92852
CONM2   1216    10802           77.92852
CONM2   1217    10805           77.92852
CONM2   1218    10902           77.92852
CONM2   1219    10905           77.92852
CONM2   1220    11002           38.96426
CONM2   1221    11005           38.96426


$...1...|...2...|...3...|...4...|...5...|...6...|...7...|...8...|...9...|..10...
CONM2   1300    20002   -1      328.33360.0762  6.2484  0.0             +1301
+1301   0.0             68.25133                0.0

$...1...|...2...|...3...|...4...|...5...|...6...|...7...|...8...|...9...|..10...
```

Aerodynamic Panel for Doublet-Lattice Theory

```
CAERO1  101001  100000                                  101     151     1       +
+       -0.6404 0.      0.0     2.5     -0.6404 6.096   0.0     2.5
```

Geometry Definition

```
$...1...|...2...|...3...|...4...|...5...|...6...|...7...|...8...|...9...|..10...
PAERO1  100000
$...1...|...2...|...3...|...4...|...5...|...6...|...7...|...8...|...9...|..10...
```

List of Span Division Points

```
AEFACT  101     0.      0.05    0.1     0.15    0.2     0.25    0.3     +
+       0.35    0.4     0.45    0.5     0.54    0.58    0.62    0.66    +
+       0.7     0.72    0.74    0.76    0.78    0.8     0.82    0.84    +
+       0.86    0.88    0.9     0.92    0.94    0.96    0.98    1.0
$...1...|...2...|...3...|...4...|...5...|...6...|...7...|...8...|...9...|..10...
```

List of Chord Division Points

```
AEFACT  151     0.      0.02    0.04    0.06    0.08    0.1     0.12    +
+       0.14    0.16    0.18    0.2     0.22    0.24    0.26    0.28    +
+       0.3     0.32    0.34    0.36    0.38    0.4     0.45    0.5     +
+       0.54    0.58    0.62    0.66    0.7     0.72    0.74    0.76    +
+       0.78    0.8     0.82    0.84    0.86    0.88    0.9     0.92    +
+       0.94    0.96    0.98    1.0
$...1...|...2...|...3...|...4...|...5...|...6...|...7...|...8...|...9...|..10...
```

Surface Spline for Interpolating Forces

```
SPLINE1 150000  101001  101001  102260  111111
```

```
SET1    111111  10000   10001   10002   10100   10101   10102   10200   +
+       10201   10202   10300   10301   10302   10400   10401   10402   +
+       10500   10501   10502   10600   10601   10602   10700   10701   +
+       10702   10800   10801   10802   10900   10901   10902   11000   +
+       11001   11002
        List of structural grid points for the spline

$
$ Modal Analysis
$
$...1...|...2...|...3...|...4...|...5...|...6...|...7...|...8...|...9...|..10...

Real Eigenvalue Extraction Method: Lanczos
EIGRL   200     0.0     50.                                     MASS
$              Frequency range of interest              Normalize to unit value of the generalized mass


$...1...|...2...|...3...|...4...|...5...|...6...|...7...|...8...|...9...|..10...
$                       VELOCITY  REFC    RHOREF  SIMXZ
AERO                    100.      2.5     1.0     +1      0
                Basic parameters for unsteady aerodynamics

$
$...1...|...2...|...3...|...4...|...5...|...6...|...7...|...8...|...9...|..10...
Flutter Data            METHOD  DENS    MACH    VEL     IMETH   Number of modes
FLUTTER 300             PKNL    100     200     300             6
                      PK Method   Pointers to FLFACTs
                      No Looping

$...1...|...2...|...3...|...4...|...5...|...6...|...7...|...8...|...9...|..10...
Mach Number - Frequency Table  for Aerodynamic Matrix Calculation

MKAERO1  0.8                                                             +
+        0.001   0.005   0.01    0.02    0.03    0.04    0.05    0.06    +
MKAERO1  0.8                                                             +
+        0.07    0.08    0.1     0.2     0.3     0.5     0.75    1.
$ MACH
$...1...|...2...|...3...|...4...|...5...|...6...|...7...|...8...|...9...|..10...

Mach Numbers for Flutter Analysis
FLFACT  200     0.800   0.800   0.800   0.800   0.800   0.800   0.800   +
+       0.800   0.800   0.800   0.800   0.800   0.800   0.800   0.800   +
+       0.800   0.800   0.800   0.800   0.800   0.800   0.800   0.800   +
+       0.800   0.800   0.800   0.800   0.800   0.800   0.800   0.800   +
+       0.800   0.800   0.800   0.800   0.800   0.800   0.800   0.800   +
+       0.800   0.800   0.800   0.800   0.800   0.800   0.800   0.800   +
+       0.800   0.800   0.800   0.800   0.800   0.800   0.800   0.800   +
+       0.800   0.800   0.800   0.800   0.800   0.800   0.800   0.800   +
+       0.800   0.800   0.800   0.800   0.800   0.800   0.800   0.800   +
+       0.800   0.800   0.800   0.800   0.800   0.800   0.800   0.800   +
+       0.800   0.800   0.800   0.800   0.800   0.800   0.800   0.800   +
+       0.800   0.800   0.800   0.800   0.800   0.800   0.800   0.800   +
+       0.800   0.800   0.800   0.800   0.800   0.800   0.800   0.800   +
+       0.800   0.800   0.800   0.800   0.800   0.800   0.800   0.800   +
+       0.800   0.800   0.800   0.800   0.800   0.800   0.800   0.800   +
+       0.800   0.800   0.800   0.800   0.800   0.800   0.800   0.800   +
+       0.800   0.800   0.800   0.800   0.800   0.800   0.800   0.800   +
+       0.800   0.800   0.800   0.800   0.800   0.800   0.800   0.800   +
+       0.800   0.800   0.800   0.800   0.800   0.800   0.800   0.800   +
+       0.800   0.800   0.800   0.800   0.800   0.800   0.800   0.800   +
+       0.800   0.800
$ DENSITY

Density Ratios for Flutter Analysis
FLFACT  100     0.0132  0.0136  0.0141  0.0145  0.0150  0.0154  0.0159  +
+       0.0164  0.0169  0.0175  0.0180  0.0186  0.0192  0.0198  0.0204  +
+       0.0210  0.0217  0.0224  0.0231  0.0238  0.0246  0.0254  0.0262  +
+       0.0270  0.0279  0.0288  0.0297  0.0306  0.0316  0.0326  0.0337  +
+       0.0348  0.0359  0.0370  0.0382  0.0395  0.0407  0.0420  0.0434  +
+       0.0448  0.0463  0.0478  0.0493  0.0509  0.0526  0.0543  0.0560  +
+       0.0579  0.0597  0.0617  0.0637  0.0658  0.0679  0.0702  0.0725  +
```

```
+       0.0748  0.0773  0.0798  0.0825  0.0852  0.0880  0.0909  0.0938  +
+       0.0968  0.0999  0.1031  0.1064  0.1098  0.1133  0.1170  0.1207  +
+       0.1246  0.1286  0.1327  0.1369  0.1413  0.1458  0.1505  0.1553  +
+       0.1603  0.1655  0.1708  0.1762  0.1819  0.1877  0.1937  0.1999  +
+       0.2063  0.2129  0.2197  0.2268  0.2340  0.2415  0.2493  0.2573  +
+       0.2655  0.2740  0.2828  0.2918  0.3012  0.3108  0.3208  0.3311  +
+       0.3417  0.3526  0.3639  0.3735  0.3830  0.3928  0.4027  0.4129  +
+       0.4232  0.4337  0.4445  0.4554  0.4665  0.4779  0.4894  0.5012  +
+       0.5131  0.5253  0.5378  0.5504  0.5633  0.5763  0.5897  0.6032  +
+       0.6170  0.6311  0.6453  0.6599  0.6746  0.6897  0.7049  0.7205  +
+       0.7363  0.7523  0.7686  0.7852  0.8021  0.8193  0.8367  0.8544  +
+       0.8724  0.8907  0.9092  0.9281  0.9473  0.9667  0.9865  1.0066  +
+       1.0270  1.0477  1.0687  1.0900  1.1117  1.1337  1.1560  1.1787  +
+       1.2017  1.2250
$
$VELOCITY
```

Velocities for Flutter Analysis

```
FLFACT  300     242.54  242.44  242.33  242.22  242.12  242.01  241.91  +
+       241.80  241.69  241.59  241.48  241.37  241.27  241.16  241.05  +
+       240.95  240.84  240.73  240.63  240.52  240.41  240.31  240.20  +
+       240.09  239.98  239.88  239.77  239.66  239.55  239.45  239.34  +
+       239.23  239.12  239.02  238.91  238.80  238.69  238.59  238.48  +
+       238.37  238.26  238.15  238.05  237.94  237.83  237.72  237.61  +
+       237.51  237.40  237.29  237.18  237.07  236.96  236.85  236.75  +
+       236.64  236.53  236.42  236.31  236.20  236.09  236.09  236.09  +
+       236.09  236.09  236.09  236.09  236.09  236.09  236.09  236.09  +
+       236.09  236.09  236.09  236.09  236.09  236.09  236.09  236.09  +
+       236.09  236.09  236.09  236.09  236.09  236.09  236.09  236.09  +
+       236.09  236.09  236.09  236.09  236.09  236.09  236.09  236.09  +
+       236.09  236.09  236.09  236.09  236.09  236.09  236.09  236.09  +
+       236.09  236.09  236.09  236.80  237.51  238.21  238.91  239.61  +
+       240.31  241.00  241.69  242.38  243.07  243.76  244.44  245.13  +
+       245.81  246.49  247.17  247.84  248.52  249.19  249.86  250.53  +
+       251.19  251.86  252.52  253.18  253.84  254.50  255.16  255.81  +
+       256.46  257.11  257.76  258.41  259.06  259.70  260.35  260.99  +
+       261.63  262.27  262.90  263.54  264.17  264.80  265.44  266.07  +
+       266.69  267.32  267.94  268.57  269.19  269.81  270.43  271.05  +
+       271.66  272.28
$
ENDDATA
```

9.2 Aerodynamic mesh for flutter analysis

In order to carry out the flutter analysis of the wing, the Doublet-Lattice Method is used to calculate the aerodynamic unsteady forces. This method requires the wing to be divided into panel elements. The aerodynamic mesh of the model is show in Figure 9.1. The mesh has 10 sections along the chord following a cosinus distribution law and sixteen sections along the span following an exponential distribution law.

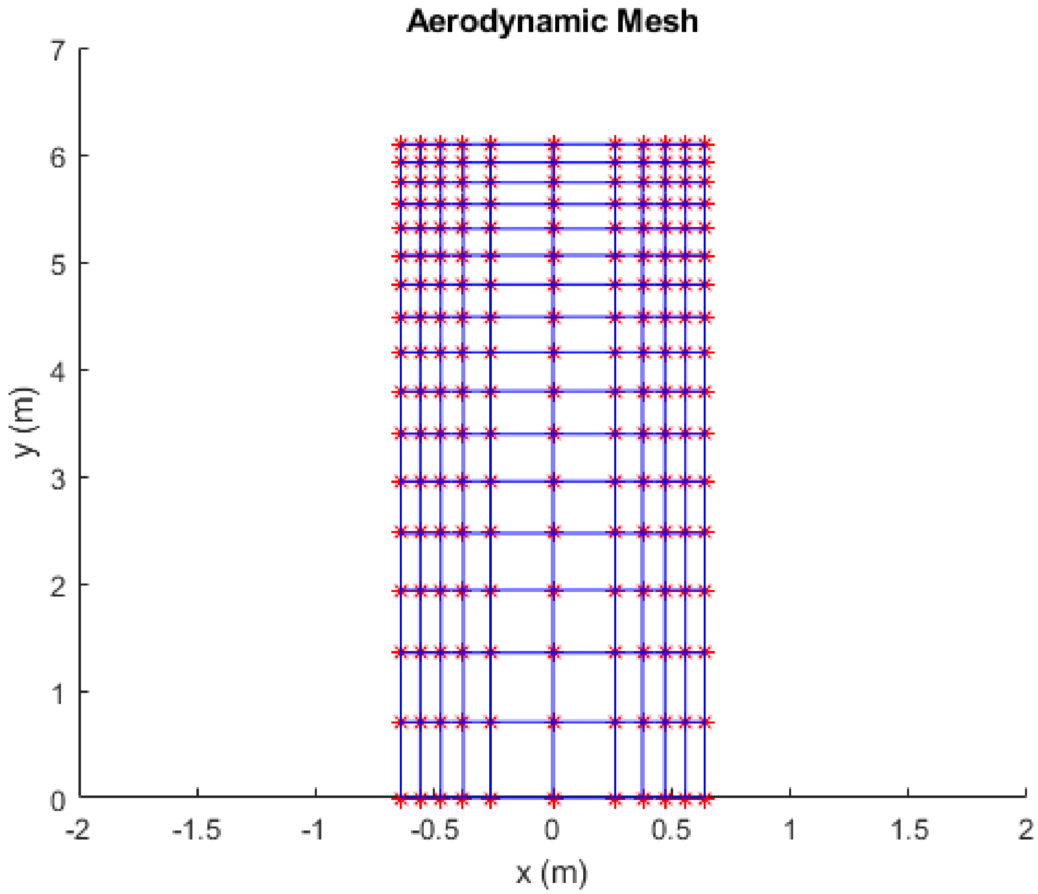

Figure 9.1: Aerodynamic Mesh.

9.3 Matlab-Nastran Interface

9.3.1 Description

An interface has been developed along this project in order to link Matlab and Nastran. This interface allows users to do a modal parametric analysis and a flutter parametric analysis in a user-friendly environment. Matlab is the software in charge of the parametric analysis and Nastran is in charge of the structural-dynamics and aeroelastic simulations.

The interface has been programmed using Matlab and it has the following functions:

1. Create .bdf input file for a SOL103 analysis in Nastran of the wing box model for different values of k_v and k_θ.
2. Create .bdf input file for a SOL145 analysis in Nastran of the wing box model for different values of k_v and k_θ, aerodynamic mesh and flight conditions(M_∞,h).
3. Execute Nastran by loading a .bdf input file.
4. Read .f06 results file from a SOL103 analysis in Nastran and get natural frequencies and displacements of desired nodes of the model.
5. Read .f06 results file from a SOL145 analysis in Nastran, plot V-g and V-f diagrams, get the static divergence speed and get the flutter speed of the model.

9.3.2 Interface Schematic

The interface can be described by the following schematic:

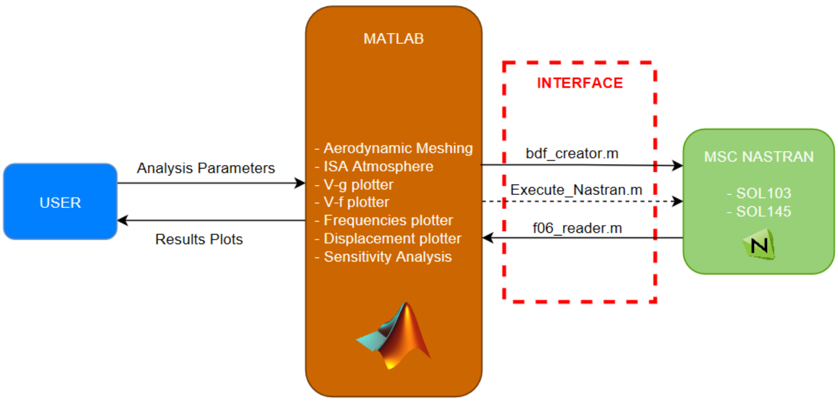

Figure 9.2: Interface Functional Schematic

9.4 Matlab code used to obtain modal response analysis for a range of k_v and k_θ

```
function calculate_dynamic_response_Main

k_f = logspace(0,7,60);
k_th=logspace(0,7,60);

frec_all_modes = zeros(4,length(k_f),length(k_th));
v20001_allmodes = zeros(4,length(k_f),length(k_th)); %Vertical
    displacements node 2001
v20005_allmodes = zeros(4,length(k_f),length(k_th)); %Vertical
    displacements node 2005
th20001_allmodes = zeros(4,length(k_f),length(k_th)); %Twist node
    20001
th20005_allmodes = zeros(4,length(k_f),length(k_th)); %Twist node
    20005
ratio_v_mode1 = zeros(length(k_f),length(k_th));
ratio_v_mode2 = zeros(length(k_f),length(k_th));
ratio_th_mode1 = zeros(length(k_f),length(k_th));
ratio_th_mode2 = zeros(length(k_f),length(k_th));

for j=1:length(k_th)
    for i=1:length(k_f)
        %Change the value of stiffnesses k_f and k_th in the bdf
            file
        change_bdf(k_f(i),k_th(j));
        %Run Nastran with the new bdf file
        run_Nastran
        %Read f06 file to obtain modes frequencies and
            eigenvector values
        %in node 20001(pod) and node 20005 (wing)
        [frec,u20001,u20005] = f06_reader('
            modos_propios_muelles_sinPunch_editado.f06');
        frec_all_modes(:,i,j) = frec;
        v20001_allmodes(:,i,j) = u20001(:,1);
        v20005_allmodes(:,i,j) = u20005(:,1);
        th20001_allmodes(:,i,j) = u20001(:,2);
        th20005_allmodes(:,i,j) = u20005(:,2);
    end
```

```
end

v_20001_mode1 = zeros(length(k_f),length(k_th));
v_20001_mode1(:,:) = v20001_allmodes(1,:,:);
v_20005_mode1 = zeros(length(k_f),length(k_th));
v_20005_mode1(:,:) = v20005_allmodes(1,:,:);
frec_mode1(:,:) = zeros(length(k_f),length(k_th));
frec_mode1(:,:) = frec_all_modes(1,:,:);
frec_mode2(:,:) = zeros(length(k_f),length(k_th));
frec_mode2(:,:) = frec_all_modes(2,:,:);
ratio_v_mode1(:,:) = v20001_allmodes(1,:,:)./v20005_allmodes
    (1,:,:);
ratio_v_mode2(:,:) = v20001_allmodes(2,:,:)./v20005_allmodes
    (2,:,:);
ratio_th_mode1(:,:) = th20001_allmodes(1,:,:)./th20005_allmodes
    (1,:,:);
ratio_th_mode2(:,:) = th20001_allmodes(2,:,:)./th20005_allmodes
    (2,:,:);

figure
mesh(k_f,k_th,ratio_v_mode1),
set(gca,'XScale','log');
set(gca,'YScale','log');
set(gca,'ZScale','log');
title('First mode vertical displacements response')
xlabel('k_{\theta}(Nm/rad)'), ylabel('k_v(N/m)'),zlabel('v_{pod}/
    v_{wing}'),

figure
mesh(k_f,k_th,ratio_th_mode2),
set(gca,'XScale','log');
set(gca,'YScale','log');
set(gca,'ZScale','log');
title('Second mode torsional response')
xlabel('k_{\theta}(Nm/rad)'), ylabel('k_v(N/m)'),zlabel('\theta_{
    pod}/\theta_{wing}'),

figure
mesh(k_f,k_th,frec_mode1),
set(gca,'XScale','log');
```

```
set(gca,'YScale','log');
title('First mode frequency')
xlabel('k_{\theta}(Nm/rad)'), ylabel('k_v(N/m)'),zlabel('First
    mode frequency $\displaystyle(\frac{rad}{s})$','interpreter','
    latex'),

figure
mesh(k_f,k_th,frec_mode2),
set(gca,'XScale','log');
set(gca,'YScale','log');
title('Second mode frequency')
xlabel('k_{\theta}(Nm/rad)'), ylabel('k_v(N/m)'),zlabel('Second
    mode frequency $\displaystyle(\frac{rad}{s})$','interpreter','
    latex'),
end

function change_bdf(k_f,k_th) %Changes value of stiffnesses k_f
    and k_th in the bdf file
fileID = fopen('modos_propios_muelles_sinPunch_parte1.bdf','r');
A=fscanf(fileID,'%c');
fclose(fileID);
fileID = fopen('modos_propios_muelles_sinPunch_parte2.bdf','r');
B=fscanf(fileID,'%c');
fclose(fileID);
fileID = fopen('modos_propios_muelles_sinPunch_editado.bdf','w');
k_f_string=num2str(k_f,'%.2E');
k_th_string=num2str(k_th,'%.2E');
s_fl=['CELAS2  2105    ',k_f_string,'20005   3       20001   3  '
    ];
s_tor=['CELAS2  2106    ',k_th_string,'20005   5       20001   5
        '];

fprintf(fileID,'%s\n',A);
fprintf(fileID,'%s\n',s_fl);
fprintf(fileID,'%s\n',s_tor);
fprintf(fileID,'%s\n',B);
fclose(fileID);
end

function run_Nastran
```

```
%Delete previous Nastran results file and order nastran to run a
%new analysis with the new bdf file
delete('C:\Users\Alfonso\Documents\universidad\master\2_Cuatrimestre\Aeroelasticidad Avanzada\Trabajo\Apartado4\modos_propios_muelles_sinPunch_editado.f04');
delete('C:\Users\Alfonso\Documents\universidad\master\2_Cuatrimestre\Aeroelasticidad Avanzada\Trabajo\Apartado4\modos_propios_muelles_sinPunch_editado.f06');
delete('C:\Users\Alfonso\Documents\universidad\master\2_Cuatrimestre\Aeroelasticidad Avanzada\Trabajo\Apartado4\modos_propios_muelles_sinPunch_editado.log');
%Run Nastran
status = system('C:\MSC.Software\MSC_Nastran_and_Patran_Student_Editions\20190\Nastran\bin\nastranw.exe modos_propios_muelles_sinPunch_editado.bdf');
%Gives time to nastran to generate the result files
pause(6)
end

function [frec,u20001,u20005] = f06_reader(filename)
A = fileread(filename);
u20005_index = strfind(A,'20005        G');
u20001_index = strfind(A,'20001        G');
u20005_matrix = zeros(4,6);
u20001_matrix = zeros(4,6);
for i=1:4
    u20005_matrix(i,:) = str2num(A(u20005_index(i)+17:u20005_index(i)+105));
    u20001_matrix(i,:) = str2num(A(u20001_index(i)+17:u20001_index(i)+105));
end
frequency_index = strfind(A,'STIFFNESS');
frec_matrix = str2num(A((frequency_index(1)+10):(frequency_index(1)+10+121*4)));
frec = frec_matrix(:,4);
u20001 = u20001_matrix(:,[3,5]);
u20005 = u20005_matrix(:,[3,5]);
end
```

Bibliography

[1] Frahm, H. Device for damping vibrations of bodies.

[2] Hodges, D., and Alvin Pierce, G. Introduction to structural dynamics and aeroelasticity.

[3] Krenk, S., and Høgsberg, J. Tuned mass absorber on a flexible structure.